


RESEARCH ARTICLE

Open Access



Plancitoxin-1 mediates extracellular trap evasion by the parasitic helminth *Trichinella spiralis*

Jing Ding¹ , Ning Xu¹, Jing Wang¹, Yushu He¹, Xuelin Wang¹, Mingyuan Liu^{1*†} and Xiaolei Liu^{1*†}

Abstract

Background *Trichinella spiralis* (*T. spiralis*) is a parasitic helminth that causes a globally prevalent neglected zoonotic disease, and worms at different developmental stages (muscle larvae, adult worms, newborn larvae) induce immune attack at different infection sites, causing serious harm to host health. Several innate immune cells release extracellular traps (ETs) to entrap and kill most pathogens that invade the body. In response, some unicellular pathogens have evolved a strategy to escape capture by ETs through the secretion of nucleases, but few related studies have investigated multicellular helminths.

Results In the present study, we observed that ETs from neutrophils capture adult worms of *T. spiralis*, while ETs from macrophages trap muscle larvae and newborn larvae, and ETs had a killing effect on parasites in vitro. To defend against this immune attack, *T. spiralis* secretes plancitoxin-1, a DNase II-like protein, to degrade ETs and escape capture, which is essential for the survival of *T. spiralis* in the host.

Conclusions In summary, these findings demonstrate that *T. spiralis* escapes ET-mediated capture by secreting deoxyribonuclease as a potential conserved immune evasion mechanism, and plancitoxin-1 could be used as a potential vaccine candidate.

Keywords *Trichinella spiralis*, Extracellular traps, Nuclease, Immune evasion, Vaccine candidate

Background

Trichinellosis is a globally common disease caused by the parasitic nematode *Trichinella spiralis* (*T. spiralis*), a type of helminth that affects mammals, particularly domestic pigs. Humans become infected by eating raw or

undercooked meat containing infectious larvae (muscle larvae, ML), which mature in the intestinal tract of the host and embed into epithelial cells of the small intestine, where females and males mate [1]. Newborn larvae (NBL) are produced by female adults, invade the bloodstream, reach muscle fibers, mature in muscles into ML, and survive for a long time [1]. Although *T. spiralis* has a large impact on public health, there is currently no effective vaccine, which requires an improved understanding of the host immune response and the immune evasion mechanisms of *T. spiralis*.

The excretory/secretory (ES) products of *T. spiralis* play an important role in invasion and immune evasion at different developmental stages, especially proteases such as serine protease [2], aspartic protease [3], and cysteine protease [4]. Some protease inhibitors have also

[†]Mingyuan Liu and Xiaolei Liu contributed equally to this work.

*Correspondence:
Mingyuan Liu
liumy36@163.com
Xiaolei Liu
liuxlei@163.com

¹ State Key Laboratory for Diagnosis and Treatment of Severe Zoonotic Infectious Diseases, Key Laboratory for Zoonosis Research of the Ministry of Education, Institute of Zoonosis, and College of Veterinary Medicine, Jilin University, Changchun 130062, China



been discovered in the ES and have been proven to play a role in invasion [5] and immune regulation [6]. In addition to proteases, the ES was also found to exhibit nuclease activity as early as 1999, and the properties of the nucleases are similar to those of DNase II [7], but their role in the parasitic process of *T. spiralis* remains unclear.

Many studies have found that innate immune cells, such as neutrophils [8] and macrophages [9], can release extracellular traps (ETs) to capture pathogens and thus limit their spread in the host. Soon after the discovery of ETs, some unicellular pathogens, such as bacteria [10–14], fungi [15], and protozoa [16], were found to escape capture by ETs through the secretion of nucleases. However, very few reports have investigated whether multicellular pathogens can trigger the release of ETs, and whether multicellular pathogens secrete nucleases to escape the capture of ETs is unclear. We hypothesize that upon infection with *T. spiralis*, the innate immune cells of the host can also capture the pathogen by releasing ETs, and the nuclease in *T. spiralis* ES will play a role in this process by degrading ETs, evading capture, and acting as a “weapon” to achieve parasitism.

Although many studies have attempted to identify nucleases in the ES, the characteristics of these nucleases have not yet been resolved. In further research, many DNase II family proteins have been discovered, but whether these proteins have nuclease activity remains controversial [17]. Therefore, this study aimed to determine whether *T. spiralis* infection can stimulate innate immune cells to release ETs, whether *T. spiralis* can escape the capture of ETs by secreting nucleases, and which components of ES exert nuclease activity. In this study, we found that neutrophils and macrophages stimulated by live *T. spiralis* worms release ETs that capture and kill the worms. Meanwhile, the role of plancitoxin-1

in degrading the DNA scaffold of ETs was also elucidated, demonstrating that multicellular pathogens take the same approach as unicellular pathogens to escape ET capture by releasing nucleases.

Results

T. spiralis induces the release of ETs

Although eosinophilia is a hallmark of parasitic infection, changes in neutrophil numbers cannot be ignored. To examine the changes in neutrophils after *T. spiralis* infection, a blood analysis was performed in infected and noninfected C57BL mice at different time points. The results showed that the portion of neutrophils increased significantly in mice infected with *T. spiralis* compared with that in the controls (Fig. 1A). Similar results were obtained for intestinal tissues in which Ly6G-positive cells, a marker that could indicate an increase in the neutrophil population, were increased in abundance in infected mice compared with noninfected mice (Fig. 1B).

To investigate the function of enriched neutrophils and to determine whether neutrophil extracellular traps (NETs) can be released to capture *T. spiralis*, polymorphonuclear neutrophils (PMNs) were isolated from mouse bone marrow and identified by flow cytometry and nuclear morphological observation. The flow cytometry analysis results showed that Ly6G + CD11b + cells accounted for more than 85% of the total isolated cells (Additional file 1: Fig. S1A shows a representative example with a purity of 87.14%). Under a fluorescence microscope, the cells with a lobular nucleus in each field accounted for approximately 90% (Additional file 1: Fig. S1B), which indicated that neutrophils were successfully isolated with high purity.

Then, PMNs were cocultured with different developmental stages in serum-free culture medium due to the

(See figure on next page.)

Fig. 1 Neutrophils release NETs in response to *T. spiralis* adults. **A** Neutrophil counts of mice at 0, 3, 7, 15, and 30 days after infection with 300 muscle larvae. Data (mean ± SD) were collected from two independent experiments ($n = 3$ mice/time point), *** ($P < 0.001$) in one way ANOVA test. **B** Representative microphotographs showing Ly6G-immunopositive cells (corresponding to neutrophils, black arrows) in the small intestine of control and infected mice at 3 dpi; scale bar: 20 μm . Data (mean ± SD) are representative of two independent experiments performed ($n = 3$ mice/group), *** ($P < 0.001$) in Student's *t* test. **C** The components of NETs induced by adults of *T. spiralis* include histone 3 (H3), myeloperoxidase (MPO), and neutrophil elastase (NE). Fifty adult worms were cocultured with 2×10^5 PMNs in medium containing ATA for 3 h at 37 °C in 5% CO₂. H3, MPO, and elastase were detected by immunofluorescence and are shown in red. The DNA scaffold of NETs and the nuclei of dead cells were dyed green with SYTOX Green, and the nuclei of all cells were dyed blue with Hoechst 33,342. Scale bar, 40 μm . **D** Live adults but not dead worms induced NETs. Fifty live adults and 50 dead adults were cocultured with PMNs separately. The culture method and staining method were the same as in **C**. NETs were dyed green, as shown in the white square. Scale bar, 80 μm . Data in **C** and **D** were collected from two independent experiments ($n = 3$), and representative images are shown. **E** and **F** The NETs quantity increased with the number of adults (0, 10, 20, 40, 80 adults) and the coculture time (0, 0.5, 1, 2, 4, 5 h) (with ATA in the medium). The results are the averages of three independent experiments (mean ± SD, *** $P < 0.001$ in one-way ANOVA). **G** The DNA scaffold of NETs derived from both the nucleus and mitochondria. Fifty adult worms were cocultured with 2×10^5 PMNs in medium containing ATA for 3 h at 37 °C in 5% CO₂. The culture supernatant and the total DNA of cells of the control group and experimental group were used as templates. Marker genes of mouse nuclear genome genes (RhoH, GAPDH, Actb, Fas) and mitochondrial genome genes (Nd1, Cox1, Atp6, Cyb) were detected by PCR. Data were collected from two independent experiments ($n = 3$), and representative images are shown

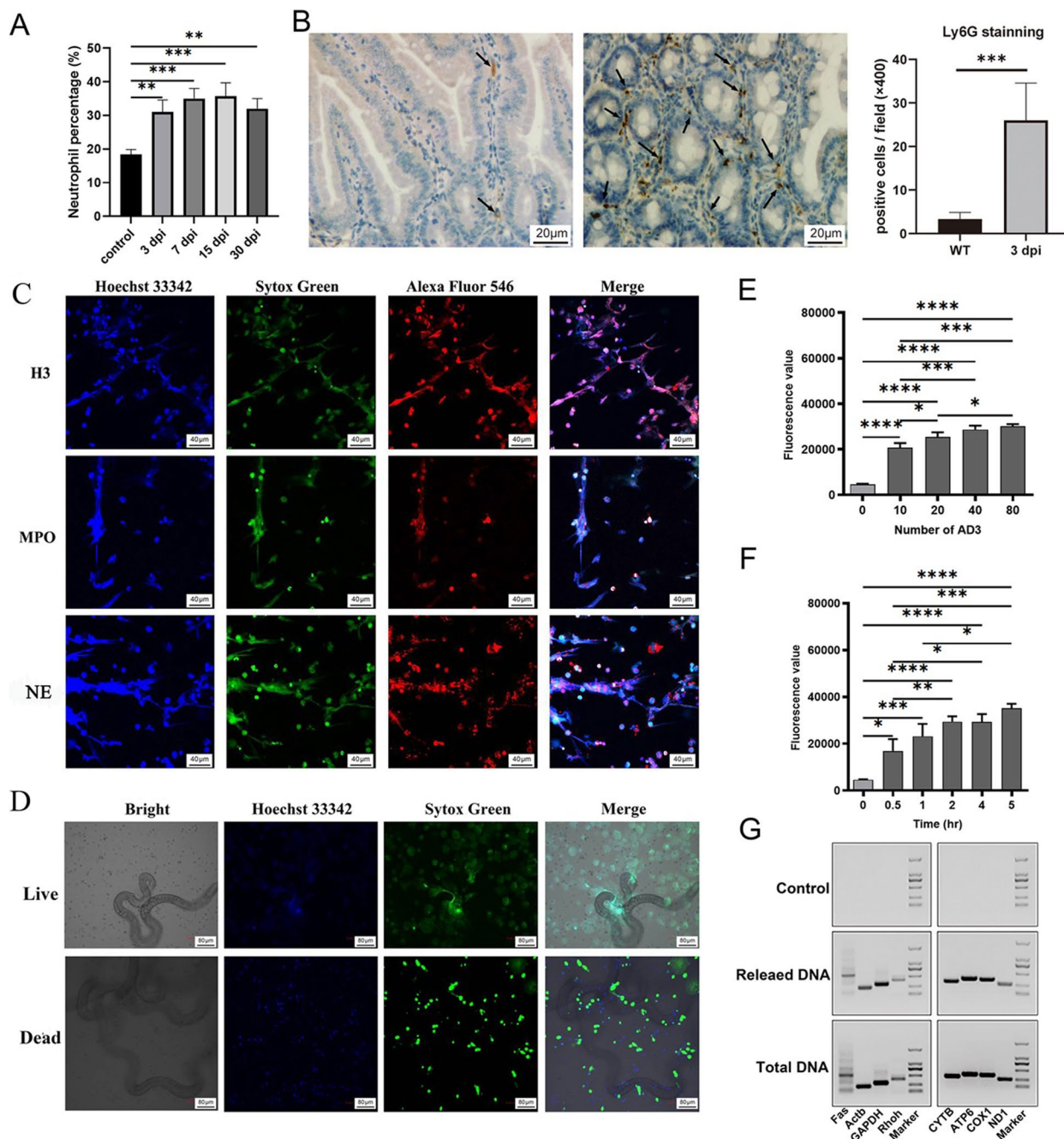


Fig. 1 (See legend on previous page.)

presence of deoxyribonuclease in serum [18]. When live AD3 (adult worms obtained at 3 days postinfection) were cocultured with PMNs, medium with or without sufficient ATA (a powerful inhibitor of ribonuclease) (as shown in Additional file 1: Fig. S1C, 25 μ M ATA could completely inhibit the nuclease activity of 10 μ g AD3 ES) was used since ES of adult worms has been reported to have nuclease activity. ATA had no effect on cell viability,

as determined by the CCK-8 assay (Additional file 1: Fig. S1D). The results showed that there were almost no spontaneously generated NETs when neutrophils were cultured alone, and NETs were not induced after cocultivation with live AD3, but NETs were formed when ATA was added to inhibit nuclease activity (Additional file 1: Fig. S1F), demonstrating that the *T. spiralis*-secreted nuclease affects the production of NETs. However, when

muscle larvae and newborn larvae were cocultured with PMNs by the same method, no NETs were produced with or without ATA, PMA-induced NETs were even inhibited, and these results were identical to those found by Rios-Lopez AL et al. [19].

Next, we tested the components of NETs released by PMNs, and iconic biomolecules on NETs, such as H3, MPO, and NE, were observed under a laser scanning confocal microscope (Fig. 1C). After coculturing live and dead worms (distinguished according to Additional file 1: Fig. S1E) with PMNs separately, the results indicated that live AD3 could induce PMNs to produce large amounts of NETs (Fig. 1D), which could partially limit the movement of the worms (Additional file 2: Video S1), whereas dead adults failed to induce PMNs to produce NETs (Fig. 1D). To further identify whether the production of NETs is caused by ES or by AD3 movement, transwell plates that separate AD3 and neutrophils were used, and the results showed that, on the premise of excluding the influence of ATA, the components in the excretory and secretory products of live worms were the important reasons for the release of NETs (Additional file 1: Fig. S1G).

Subsequently, the quantity of NETs produced by PMNs cocultured with different numbers of AD3 at different time points was detected. The results showed that the quantity of NETs increased with increases in the amount of AD3 added to the plate compared with that of the control group without AD3 (Fig. 1E). In the experiment using 50 adult worms to stimulate PMNs for 5 h, we observed that NETs were formed at 0.5 h, and the quantity of NETs gradually increased over time (Fig. 1F). The results proved that NETs formed in a time- and dose-dependent manner.

To explore the source of the DNA scaffold of NETs released by neutrophils exposed to AD3, the DNA obtained from each group was used as a template, and specific amplification primers for the nuclear genes *Rhoh*, *GAPDH*, *Actb*, and *Fas* and mitochondrial genes *Nd1*, *Cox1*, *Atp6*, and *Cytb* were used for PCR amplification. The results showed that no components were amplified in the culture supernatant of the negative control group, and a total of eight gene fragments in the mitochondrial and nuclear genomes of the PMN culture supernatant of the experimental group were successfully amplified (Fig. 1G), which suggested that the DNA components of NETs induced by AD3 were derived from both nuclear and mitochondrial DNA.

ETs release is not restricted to neutrophils but has also been observed in macrophages/monocytes [9, 20]. Since *T. spiralis* adults can induce the release of NETs from neutrophils, it is also worth exploring whether other developmental stages of this worm can induce the release of METs from macrophages. To explore this issue, the

macrophage cell line J774A.1 was cocultured with ML or NBL using the same method as that used for PMNs, and the results showed that live ML could also induce METs release in medium containing ATA (Additional file 1: Fig. S1H and Fig. 2A–B), and the same result was also observed in NBL (Fig. 2C–D and Additional file 3: Video S2). In summary, the three different developmental stages of *T. spiralis* can all induce the release of ETs from innate immune cells.

Parasiticidal effect is induced by ETs and ADCP in vitro

To investigate whether *T. spiralis* is killed by ETs produced in coculture medium containing ATA, parasite survival was monitored over 12 h by microscopic observation of worm mobility and morphology. Overall, adult worms were adversely affected by NETs within this time frame, as significant differences in the number of surviving worms were observed between the exposed and non-exposed groups (Fig. 2E). Additionally, there was also a significant difference in the survival quantity of ML or NBL cocultured with J774A.1 cells compared with that of the controls (Fig. 2F–G). A restriction of worm motility caused by ET entrapment was observed (comparison between Additional file 4: Video S3 and Additional file 5: Video S4) in the meantime; therefore, we hypothesize that ETs can not only kill parasites but also restrict the spread of parasites in the host and recruit other immune cells to the infection site to attack and kill the worms in vivo.

In addition to the killing effect of METs, studies have shown that antibody-dependent cellular phagocytosis (ADCP) is a pivotal mechanism through which macrophages defend against parasites [21]. Therefore, anti-*T. spiralis* serum was added to the coculture medium of macrophages and *T. spiralis* to analyze the parasiticidal effect. The results showed that the antiserum could mediate ADCP (Fig. 3A–D and Additional file 6: Video S5), although the worms were too large for the macrophages to swallow them up, leading to an approximately 15% killing efficiency against NBL and a relatively low killing rate against ML (Fig. 3G). The NBL in the medium without antiserum were not phagocytized by macrophages (Fig. 3E–F), and it is precisely for this reason that NBL cannot be fixed onto the coverslips, and very few NBL can be observed under the scanning electron microscope. ML are much larger than NBL, so all the ML were washed off during sample preparation and cannot be observed under a scanning electron microscope.

Excretory/secretory products of *T. spiralis* degrade NETs

ETs were shown to capture worms and then kill the worms, but whether *T. spiralis* can evade capture, as other pathogens do by secreting nucleases, remains unclear. In

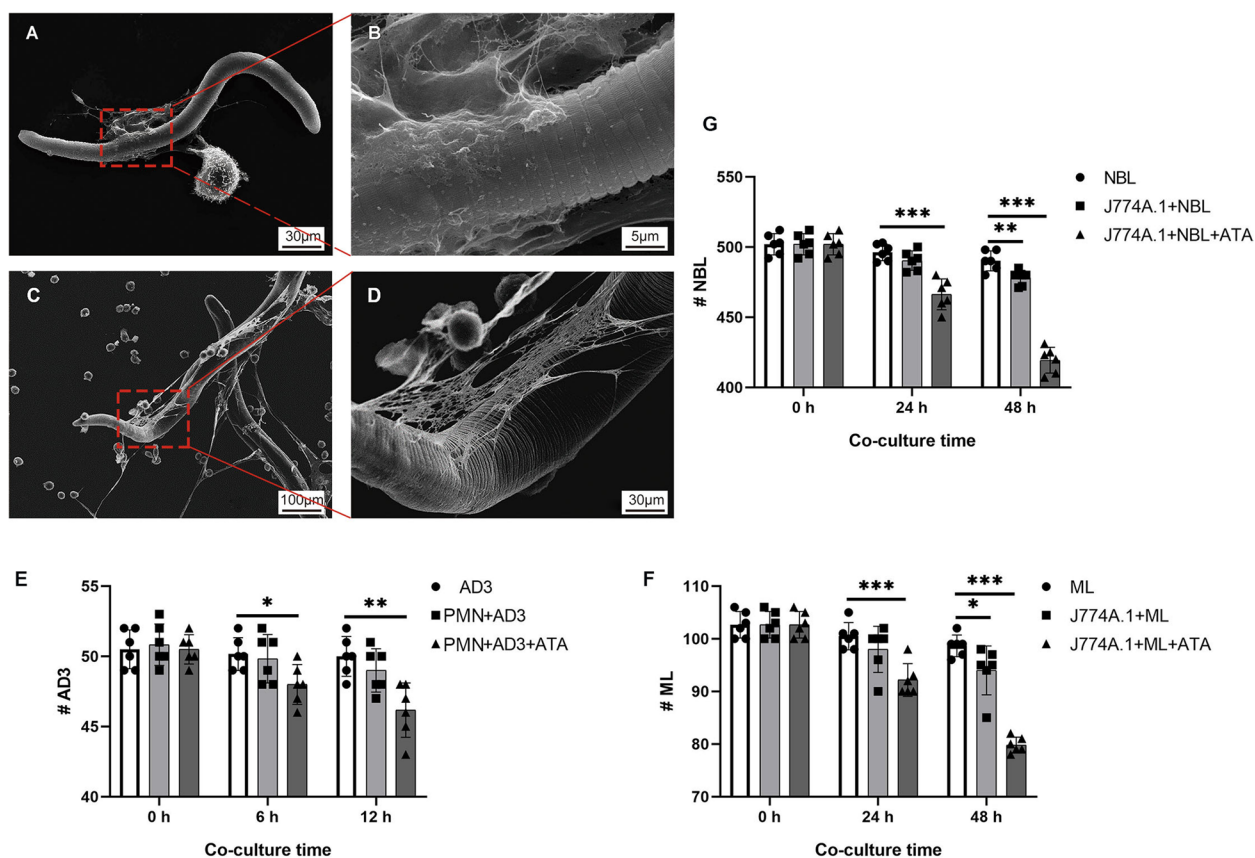


Fig. 2 Macrophages can release METs, and ETs kill *T. spiralis* in vitro. **A** and **B** Scanning electron micrographs obtained after a total of 400 newborn larvae (NBL) cocultured with 1×10^4 J774A.1 cells in medium containing ATA for 3 h at 37 °C in 5% CO₂. Scale bar, 30 μm (**A**) and 5 μm (**B**). **C** and **D** SEM micrographs obtained after 100 muscle larvae (ML) cocultured with 1×10^4 J774A.1 cells in medium containing ATA for 3 h at 37 °C in 5% CO₂. Scale bar, 100 μm (**C**) and 30 μm (**D**). Data in **A–D** were collected from two independent experiments ($n=3$), and representative images are shown. **E** Approximately 50 adults were cocultured with 2×10^5 PMNs in medium containing ATA, and the surviving worms were counted after 6 and 12 h of cocultivation. Data were collected from two independent experiments ($n=3$) and analyzed by ANOVA. **F** and **G** Approximately 100 ML (**F**) or 400 NBL (**G**) were cocultured with 1×10^4 J774A.1 cells in medium containing ATA, and the surviving worms were counted after 24 and 48 h of cocultivation. Data in **E–G** were collected from two independent experiments ($n=3$) and analyzed by one-way ANOVA. * ($P < 0.05$), ** ($P < 0.01$), and *** ($P < 0.001$) indicate a statistically significant difference

this study, we needed to observe the degradation process of NETs in still pictures, so we used PMA instead of live worms to induce the formation of NETs. AD3 ES was added to the culture medium after the induction of NETs by PMA. The NETs gradually decreased over time in the medium without ATA (Fig. 4A–B), while no change in NETs quantity was detected in the culture medium with ATA (Additional file 1: Fig. S2A). The results showed that AD3 ES exhibited the ability to degrade the DNA scaffold of NETs, which confirmed the presence of nucleases in the ES. Subsequently, AD3 ES and substrate DNA (λ DNA) were incubated to determine its nuclease activity, and 5 μg AD3 ES could significantly degrade 0.2 μg λ DNA (Additional file 1: Fig. S2B), so we used this dose in the following experiments. Then, AD3 ES were incubated with λ DNA at different pH conditions with or without metal ions, and agarose gel electrophoresis results

showed that AD3 ES exhibited nuclease activity under acidic and neutral pH conditions and that the strongest activity was at pH 5.0 (Fig. 4B). Without AD3 ES, λ DNA was not degraded under different pH conditions (Additional file 1: Fig. S2C). Additionally, the relative nuclease activity of AD3 ES was detected by the absorbance of substrate DNA at A260 nm, and the results showed that the presence or absence of divalent metal ions Ca²⁺/Mg²⁺ and EDTA did not affect the activity, which further demonstrated that the nuclease in ES meets the typical characteristics of DNase II (Fig. 4C). Moreover, ES collected at the muscle larvae stage (ML ES) and newborn larvae stage (NBL ES) also exhibited nuclease activity (Additional file 1: Fig. S3). In summary, our findings indicate that the nuclease in ES belongs to the DNase II superfamily and can degrade the NETs backbone, thereby facilitating the evasion of NETs capture.

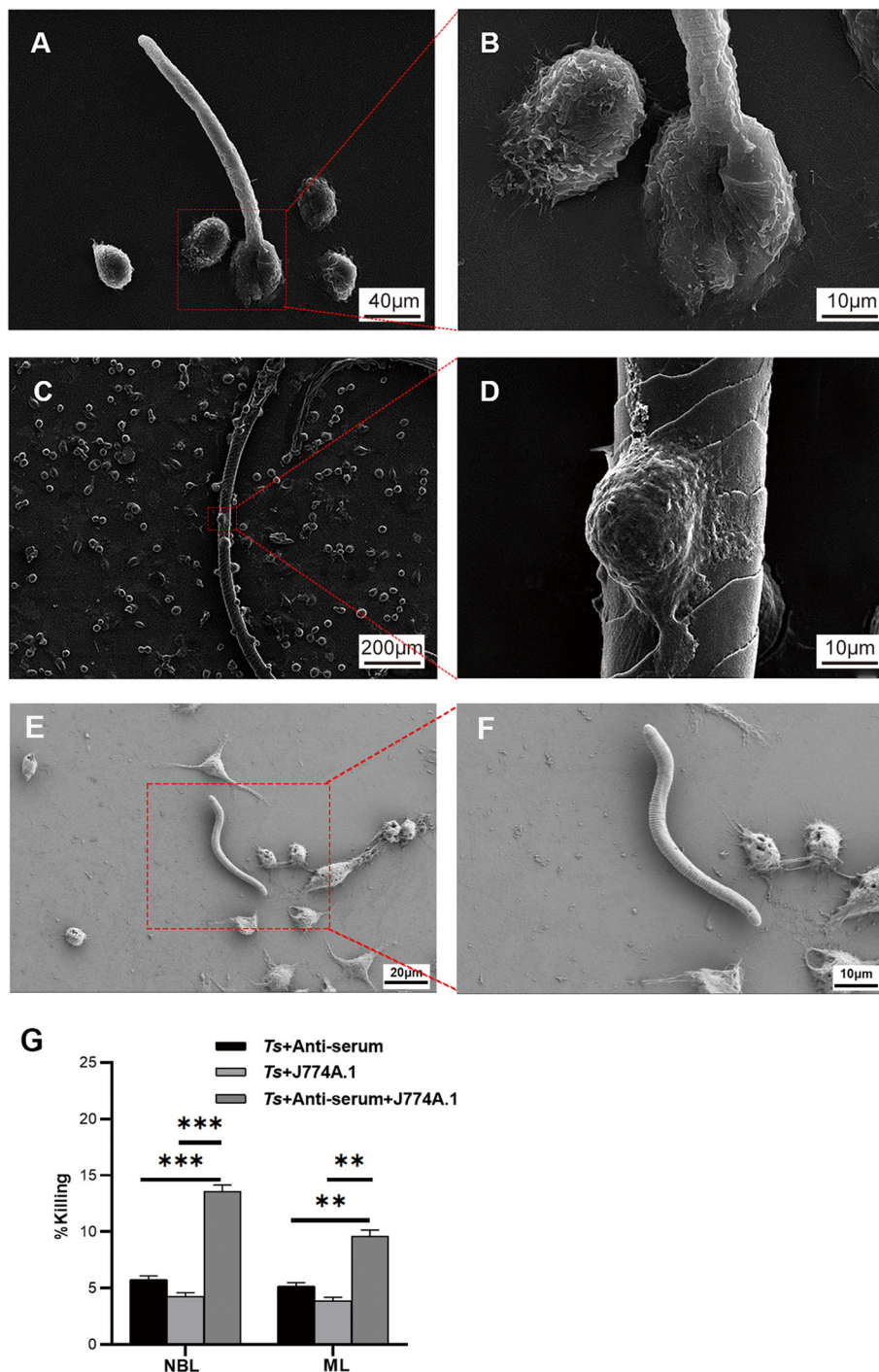


Fig. 3 The antibody-dependent cell-mediated phagocytosis effect of macrophages kills ML and NBL. **A** and **B** Scanning electron micrographs of NBL-J774A.1 cocultivations. A total of 400 newborn larvae (NBL) were cocultured with 1×10^4 J774A.1 cells with anti-*T. spiralis* serum in culture medium for 3 h at 37 °C in 5% CO₂. Scale bar, 40 μm (**A**) and 10 μm (**B**). **C** and **D** Scanning electron micrographs of ML-J774A.1 cocultivations. One hundred muscle larvae (ML) were cocultured with 1×10^4 J774A.1 cells with anti-*T. spiralis* serum for 3 h at 37 °C in 5% CO₂. Scale bar, 200 μm (**C**) and 10 μm (**D**). **E** and **F** Scanning electron micrographs of NBL-J774A.1 cocultivations. A total of 400 NBL were cocultured with 1×10^4 J774A.1 cells without anti-*T. spiralis* serum in culture medium for 3 h at 37 °C in 5% CO₂. Scale bar, 20 μm (**E**) and 10 μm (**F**). Data in **A–F** were collected from two independent experiments ($n = 3$), and the representative images are shown. **G** Killing efficiency statistics (mean \pm SD, $n = 3$, $^{***}P < 0.01$ in two-tailed Student's *t* test)

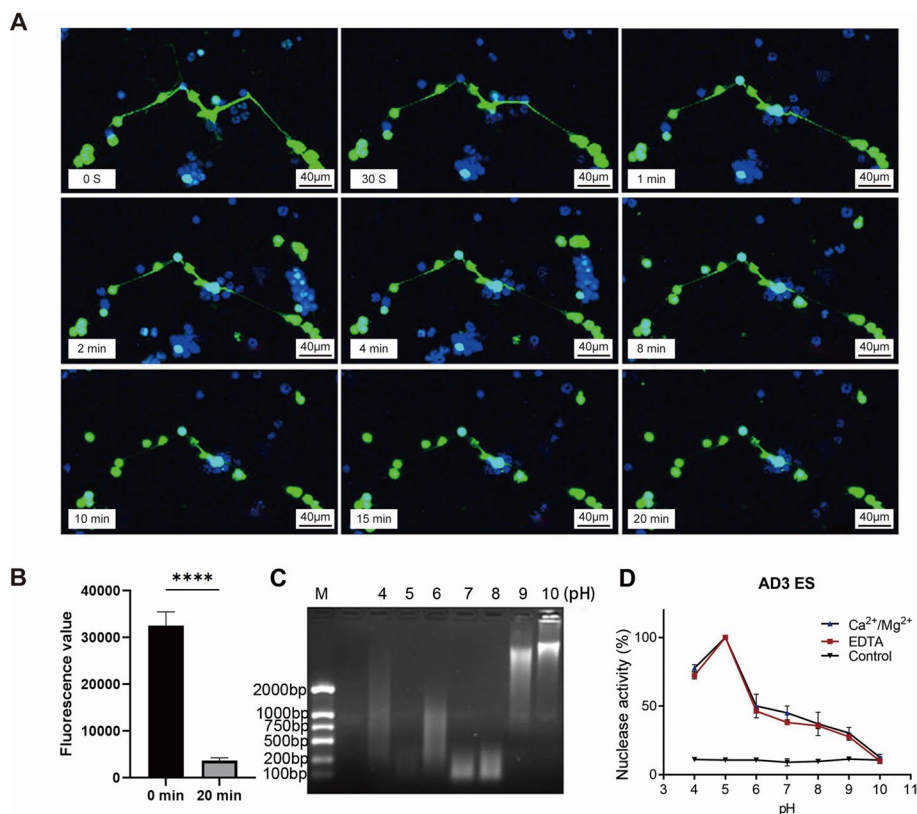


Fig. 4 Excretory/secretory products of adult worms obtained at 3 days post infection have nuclease activity to degrade NETs in vitro. **A** Images of NETs induced by PMA after the addition of excretory/secretory products of adult worms obtained at 3 days post infection (AD3 ES) in the cultivation at various time points. The DNA scaffold of NETs and the nuclei of dead cells were dyed green with SYTOX Green, and the nuclei of all cells were dyed blue with Hoechst 33,342. AD3 ES showed DNase activity in a time-dependent manner. Scale bar, 40 µm. Data were collected from two independent experiments ($n=3$), and representative images are shown. **B** Quantification of NETs detected by PicoGreen in the samples at 0 and 20 min in A. Data were collected from two independent experiments ($n=3$) and analyzed by Student's t test. **** ($P<0.0001$) indicates a statistically significant difference. **C** λ DNA was detected by agarose gel electrophoresis after reacting with AD3 ES under different pH conditions, and λ DNA was most significantly degraded at pH 5. Data were collected from two independent experiments ($n=3$), and a representative image is shown. **D** λ DNA was detected by spectrophotometry after reacting with AD3 ES under different pH conditions with or without Ca²⁺/Mg²⁺. The absorbance of λ DNA was highest at pH 5, and there was no significant difference with or without Ca²⁺/Mg²⁺ at each pH analyzed by Student's t test. Data were collected from two independent experiments ($n=3$)

Plancitoxin-1 in ES exerts nuclease activity

To isolate and identify the nuclease protein from ES, its molecular weight was determined by zymography, and a DNase band was found between 35 and 45 kDa (Fig. 5A). The band in this interval was excised and analyzed by mass spectrometry. Several DNase II family proteins detected by mass spectrometry and several nuclease family proteins previously screened in our lab were analyzed for enzyme activity domains, and all the members have conserved DNase II domains (Additional file 1: Fig. S4A), but only plancitoxin-1 (*Ts*-Pt-1) (gene ID: XM_003370715; protein ID: XP_003370763) has typical conserved enzymatic activity centers, which contain three histidine residues. Moreover, the histidine residue in the C-terminus is surrounded by a highly conserved 5-mer peptide, DHSKW [22], which

has been proposed as the core catalytic center of most DNase II family members [23] (Fig. 5B). Thus, we speculated that *Ts*-Pt-1 exerts nuclease activity in AD3 ES instead of the other proteins that do not have core catalytic centers. To verify this hypothesis, DNase II-8 (protein ID: AAY32323) and *Ts*-Pt-1 were expressed in CHO cells, and bovine DNase II expressed with the same method was used as a control. We found that recombinant DNase II-8 had no nuclease activity (Fig. 5C–D), whereas recombinant *Ts*-Pt-1 (*rTs*-Pt-1) exhibited strong nuclease activity, although the activity was inhibited by some divalent metal ions at high concentrations (Fig. 5E), which confirmed our speculation. We also demonstrated that the ML stage-specific protein P43 (GenBank No. AAA30327.1) and

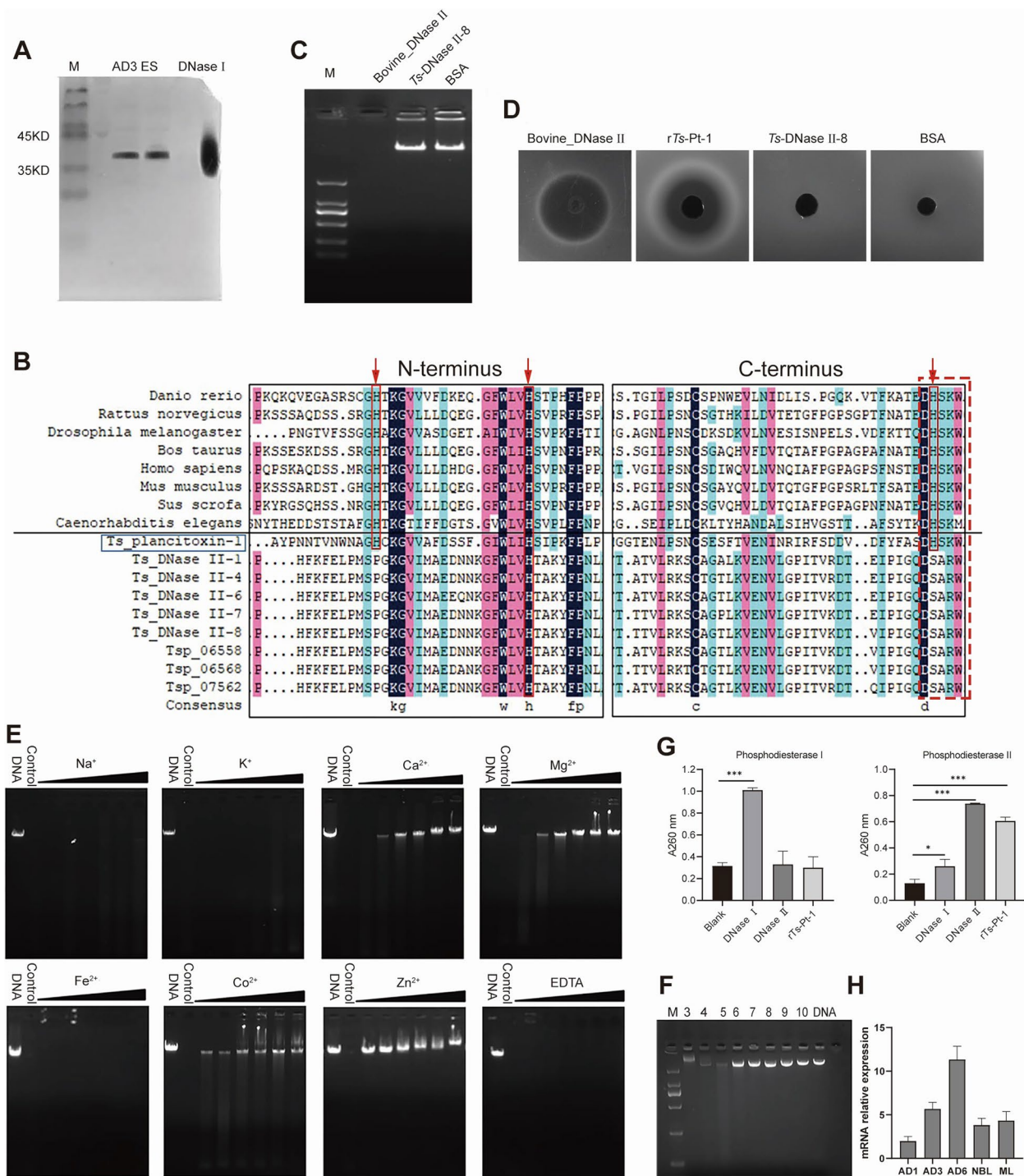


Fig. 5 Identification of nuclease-active proteins in excretory/secretory products of adult worms obtained at 3 days post infection. **A** The protein with nuclease activity in excretory/secretory products of adult worms obtained at 3 days post infection (AD3 ES) was between 35 and 45 kDa, as detected by 1D zymography. **B** All proteins obtained by mass spectrometry were blast searched, and only *Ts*-Pt-1 had typical enzymatic active sites. The protein DNase II-8, which does not have a typical enzymatic active site, had no enzymatic activity detected by agarose gel electrophoresis (**C**) or the agar diffusion method (**D**). **E** *Ts*-Pt-1 with typical enzymatic active sites had nuclease activity detected by agarose gel electrophoresis, and Ca^{2+} , Mg^{2+} , Co^{2+} , and Zn^{2+} had an inhibitory effect on its enzymatic activity in a concentration-dependent manner. **F** *Ts*-Pt-1 has the strongest enzymatic activity at pH 5, as detected by agarose gel electrophoresis. **G** The degradation products of λ DNA cleaved by *rTs*-Pt-1 can be further cleaved by phosphatidase II. Data were collected from two independent experiments ($n=3$). * ($P<0.05$) and *** ($P<0.001$) indicate a statistically significant difference analyzed by one-way ANOVA test. **H** The mRNA levels of plancitoxin-1 were highest in the adult stage, as assessed by qPCR. The ML group was regarded as 100%. The results are the averages of three independent experiments (mean \pm SD)

the NBL stage-specific protein T314 (GenBank No. AAK16519.1), which are in the *T. spiralis* DNase II family with no typical conserved enzymatic activity centers, exhibited no nuclease activity (Additional file 1: Fig. S5). The optimal pH of r*Ts*-Pt-1 was 5 (Fig. 5F), which is the same as the optimal pH of ES. The identification of the terminus of the enzymatic hydrolysates showed that r*Ts*-Pt-1 belongs to the DNase II family (Fig. 5G), and its enzyme characteristics are consistent with those of AD3 ES. Moreover, it was detected at all developmental stages (Fig. 5H). Notably, when we cloned the *Ts*-Pt-1 gene, we found that the sequence in GenBank was not complete due to the lack of the signal peptide, so we corrected it and submitted the new sequence to GenBank (gene ID: MH820373.1; protein ID: QBK17306.1). The conserved domain of the new sequence is shown in Additional file 1: Fig. S4B. A BLAST search of NCBI nonredundant protein sequences indicated that *Ts*-Pt-1 is conserved among nematodes, including *Caenorhabditis elegans*, *Brugia malayi*, *Toxocara canis*, and *Ascaris suum*. Other DNase II family proteins of *T. spiralis* without a typical enzymatic active center are in the same clade as those of *Trichuris suis* (Additional file 1: Fig. S6).

Since a small amount of death in adult worms cannot be avoided during the process of ES collection, we cannot determine whether *Ts*-Pt-1 in ES comes from live worm secretion or dead worm disintegration. Therefore, we used ES harvested from approximately 10,000 adult worms and crude proteins extracted from 30 adult worms (approximately 30 deaths per 10,000 adults) in the λ DNA degradation experiment. The nuclease activity of the ES was significantly better than that of the same amount of crude extract (Additional file 1: Fig. S7A), indicating that *Ts*-Pt-1 was secreted into the culture medium, not derived from the disintegration of dead worms. In addition, we also performed Western blotting to detect the reaction of r*Ts*-Pt-1 with sera collected from *T. spiralis*-infected mice and pigs. The results showed that r*Ts*-Pt-1 underwent an immune reaction with positive sera but not with negative sera, which proved that the protein can be secreted into the host to elicit an immune response (Additional file 1: Fig. S7B). Moreover, the immunofluorescence results showed that *Ts*-Pt-1 was observed on the teguments of adults after reaction with the anti-r*Ts*-Pt-1 antibody (Additional file 1: Fig. S8), which was additional evidence that plancitoxin-1 can be secreted.

A previous study reported that four monoclonal antibodies to phenylalanine hydroxylase exerted different effects on enzyme activity: two were inhibitory (62% and 11% inhibition, respectively), one was stimulatory (92% stimulation), and the fourth had no effect on enzyme activity [24]. To explore the effect of the anti-r*Ts*-pt-1

antibody on the nuclease activity of r*Ts*-Pt-1, the rabbit polyclonal antibody was collected, purified to remove nuclease and coincubated with r*Ts*-Pt-1 in vitro, and the nuclease activity of r*Ts*-Pt-1 was then tested. The results showed that sufficient rabbit polyclonal antibody did not completely inhibit the nuclease activity of r*Ts*-Pt-1 (Additional file 1: Fig. S7D-F), and the inhibition efficiency was approximately 53.35%. Since the enzymatic activity of plancitoxin-1 in ES cannot be completely blocked by an anti-r*Ts*-pt-1 antibody, we consider that plancitoxin-1 contributes to the nuclease activity of ES but may not be exclusively responsible for the activity.

Interference with the expression of plancitoxin-1 reduces the nuclease activity of ES and the pathogenicity of *T. spiralis*

As the antibody cannot completely inhibit nuclease activity, we performed RNAi on the worm to inhibit the expression and secretion of *Ts*-Pt-1, with the aim of investigating the effect of expression change on ES nuclease activity. The analysis of transfection by fluorescence microscopy showed that fluorescence staining was observed in ML after incubation with 2 μ M FAM-labeled control siRNA for 12 h. However, adult worms were transfected with extremely low efficiency (Fig. 6A). Therefore, we used ML to verify the effect of RNAi on nuclease activity in subsequent experiments. Although the protein expression level of *Ts*-Pt-1 in ML was lower than that in adult worms, it was detected at all developmental stages (Additional file 1: Fig. S7C), and this finding served as one of the bases for focusing on ML for RNAi. In this way, we could demonstrate the effect of *Ts*-Pt-1 knockdown on invasion during the development of infectious larvae into adults. The qPCR results showed that the *Ts*-Pt-1 gene expression level in ML treated with 2 μ M of different siRNA interference sites (siRNA-86, siRNA-290, and siRNA-920) was 74.6%, 45.1%, and 82.2% of that found in the control group, respectively (Fig. 6B). The Western blot results showed a similar inhibition of the expression levels of the *Ts*-Pt-1 protein in ML treated with 2 μ M siRNA-86, siRNA-290, and siRNA-920 compared with that in the PBS group (Fig. 6C). No significant difference in interference efficiency was found among 1, 2, and 3 μ M siRNA-290 (Fig. 6D). The abovementioned results confirm that RNAi can effectively inhibit the transcription and expression of *Ts*-Pt-1. We then selected siRNA-290, which exhibited the highest inhibition efficiency, to interfere with a large amount of ML and collected the ES of the worms after interference. No significant change was found in the activity of the worm 24 h after the interference (Fig. 6E), but the quantity of NETs in the interference group was significantly larger than that of the control group when cocultured with

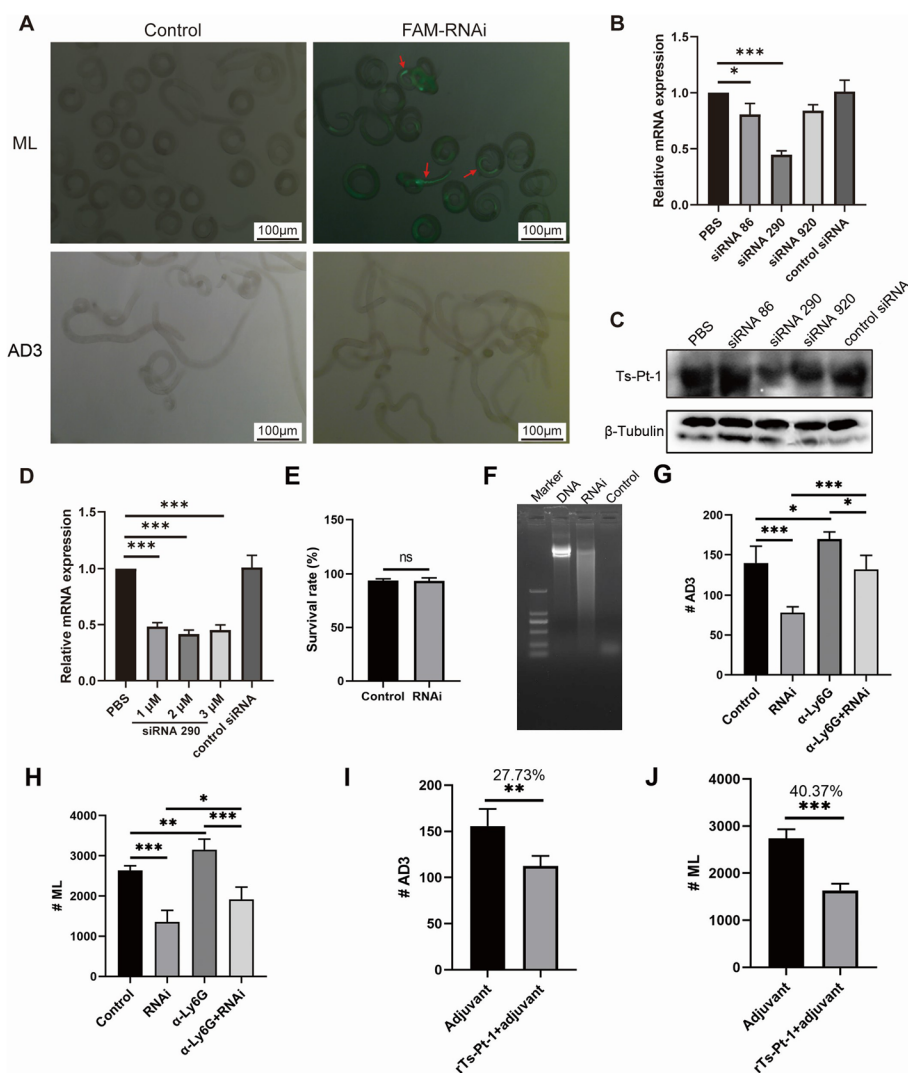


Fig. 6 *Ts-Pt-1* exerts nuclease activity in excretory/secretory products and can be a potential vaccine candidate. **A** FAM-siRNA was successfully transferred into muscle larvae (ML), and green fluorescence was observed in the intestinal tube of the worms. Scale bar, 100 μ m. qPCR (**B**) and Western blot (**C**) analysis of relative *Ts-Pt-1* expression levels after *T. spiralis* ML were transfected with two μ M siRNA86, siRNA290, and siRNA920. Data in **B** were collected from two independent experiments ($n=3$). * ($P<0.05$) and *** ($P<0.001$) indicate a statistically significant difference analyzed by one-way ANOVA. **D** qPCR analysis of relative *Ts-Pt-1* expression levels after *T. spiralis* ML were transfected with 1, 2, or 3 μ M siRNA290. Data were collected from two independent experiments ($n=3$). *** ($P<0.001$) indicates a statistically significant difference analyzed by one-way ANOVA. **E** Survival rate analysis of normal ML and *Ts-Pt-1*-RNAi-treated ML at 24 h after interference. Data were collected from two independent experiments ($n=6$ wells) and analyzed by Student's *t* test; ns indicates no significant difference. **F** The nuclease activity of ES derived from *Ts-Pt-1*-RNAi-treated ML was weaker than that of the control larvae, as detected by agarose gel electrophoresis. **G** and **H** Neutrophil-depleted mice were treated with anti-Ly6G mAb by intraperitoneal (i.p.) injection once a day $-1, 0, 1, 2,$ and 3 . On day 0, neutrophil-depleted mice and wild-type mice were infected with 200 normal ML or *Ts-Pt-1*-RNAi-treated ML. The number of adult worms collected from the intestine was counted in each group (**G**), and the number of ML collected from muscle was counted in each group (**H**). Data were collected from two independent experiments ($n=6-8$ mice/group) and analyzed by ANOVA; * ($P<0.05$), ** ($P<0.01$), and *** ($P<0.001$) indicate a statistically significant difference. **I** and **J** The number of adult worms was reduced by 27.73% in mice immunized with *rTs-pt-1* compared with the control mice (**I**). The number of ML was reduced by 40.37% in mice immunized with *rTs-pt-1* compared with control mice (**J**). Data were collected from two independent experiments ($n=6-8$ mice/group) and analyzed by students' *t* test; ** ($P<0.01$) and *** ($P<0.001$) indicate a statistically significant difference compared with the control groups

PMNs in medium without ATA (Additional file 1: Fig. S9). The results from a nuclease activity analysis showed that the nuclease activity of ES collected from worms

after interference was weaker than that found for the same amount of normal ES (Fig. 6F).

To detect whether *Ts-Pt-1* participates in the anti-neutrophil immune response in vivo and exerts an effect on

pathogenicity, mice depleted of neutrophils were infected with ML after treatment with siRNA-290, and the numbers of adults and ML were determined at 7 dpi and 35 dpi, respectively. The efficiency of cell depletion was confirmed by visualizing cellular recruitment in the small intestine (Additional file 1: Fig. S10). The results showed that the number of adult worms recovered from the intestine of mice infected with ML after interference was significantly lower than that of the control group, while once neutrophils were depleted, the number of adult worms increased significantly compared with the control or the interference group (Fig. 6G). A similar result was obtained for the number of ML (Fig. 6H), which proved that plancitoxin-1 defense against the immune response of neutrophils and that the reduction in the expression of *Ts*-Pt-1 could reduce the pathogenicity of *T. spiralis*. The above results jointly indicate that the reduction in *Ts*-Pt-1 expression directly affects the nuclease activity of ES and that plancitoxin-1 is an essential factor used by *T. spiralis* to avoid ET capture.

Immunization with r*Ts*-Pt-1 protects against infection

We further investigated the significance of r*Ts*-Pt-1-specific antibodies in host protection against parasite infection in vivo. ICR mice were immunized three times with His-tagged r*Ts*-Pt-1 and Freund's adjuvant. As expected, compared with the adjuvant group, the groups vaccinated with r*Ts*-Pt-1 exhibited a 27.73% reduction in adult worm burden and a 40.37% reduction in ML burden (Fig. 6I–J), which indicated that r*Ts*-Pt-1-specific antibodies provide protection against *T. spiralis* infection and that plancitoxin-1 can be used as a vaccine candidate.

Discussion

T. spiralis uses diverse mechanisms to escape host innate immunity, and previous studies have mainly focused on the regulation and suppression of the host immune system [25]. However, other immune evasion mechanisms are worth exploring, and the proteins involved in these processes are likely to be important virulence factors that can be explored as potential candidates for vaccine development or novel therapies. Here, we reported that *T. spiralis* could evade capture by secreting nucleases that can degrade the ET scaffold, and the protein exerting nuclease activity in excretory–secretory (ES) products can be considered a vaccine candidate.

ETs are high-concentration reticular DNA complexes that are released by activated neutrophils and macrophages in different ways. Many pathogens, including bacteria such as *Staphylococcus aureus*, fungi such as *Candida albicans*, viruses such as dengue virus and parasites, can stimulate neutrophils to produce NETs [26]. In addition to neutrophils, macrophages, eosinophils, and

mast cells have also been confirmed to release ETs [27]. To date, most studies on parasite-induced ET formation have focused on parasitic protozoa, such as *Plasmodium falciparum* [28, 29], *Toxoplasma gondii* [30], *Leishmania* [31], *Trypanosoma cruzi* [32], *Eimeria* [33], and *Neospora* [34]. In recent years, *Strongyloides stercoralis* [35], *Schistosoma japonicum* [36], *Nippostrongylus brasiliensis* [37], *Dirofilaria immitis* [38], hookworms [39], and *Litomosoides sigmodontis* [40] have been reported to induce ET release. Our findings provide new evidence supporting the notion that not only single-cell pathogens but also multicellular pathogens can induce ET formation. Bouchery et al. postulated that dead hookworms induce the release of NETs [39], while we showed the opposite results that only live worms could induce the release of NETs with ATA in the culture medium, indicating that certain components secreted by *T. spiralis* stimulated immune cells to release NETs.

Studies have shown that the DNA scaffold of ETs formed by neutrophils and mast cells is usually derived from the nuclear genome [41, 42], and the DNA scaffold of ETs formed by eosinophils is derived from the mitochondrial genome [43]. A subsequent study showed that neutrophils pretreated with GM-CSF also release mitochondrial DNA after being stimulated by some chemical factors, such as LPS and C5a [44]. In our previous research, we used mitochondrial probe labeling, PCR, and fluorescence in situ hybridization to explore the source of the DNA backbone on METs, and the results showed that DNA from both mitochondria and the nucleus can be detected on METs induced by *Candida albicans* [20]. The above research results indicate the existence of various formation mechanisms of ETs. In this study, we examined the DNA skeleton components of NETs induced by adult *T. spiralis* worms and found that both nuclear DNA and mitochondrial DNA were present, which provides additional evidence stimulating further exploration of the formation mechanism of ETs.

The bactericidal effect of NETs is limited and even controversial, depending on the pathogen, because some pathogens express virulence factors to escape capture via NETs [45]. Our results showed that ETs could partially limit the motion of the parasite and kill *T. spiralis* in vitro only when ATA was present. In comparison, the killing effect of ETs on adults was weaker than that of muscle larvae and newborn larvae, which may be due to the large size and thick cuticle of adult worms. This finding was consistent with the findings of Bouchery et al., who argued that NETs have a significant negative effect on worm vitality. In addition to the killing effect of ETs, macrophages exert antibody-dependent phagocytosis (ADCP) in the presence of antiserum and showed a slight killing effect on ML and NBL. Based on the above

results, we speculate that neutrophils cooperate with other immune cells to kill worms. Neutrophils restrict the movement of worms and recruit other immune cells, such as macrophages, to infection sites to kill worms through ADCP or other methods.

Most pathogens can be captured by ETs, but some of them have evolved different mechanisms to counteract ETs. For example, DNase has been found in some gram-positive bacterial pathogens, such as *Streptococcus pyogenes*, *Staphylococcus aureus*, and *Streptococcus pneumoniae*, and can be used to escape ETs capture because it degrades the DNA scaffold of ETs [46]. *Candida albicans* can escape from the trapping and killing of NETs by secreting DNase [47]. For protozoa, it has been reported that *Leishmania infantum* induces NETs release and that promastigotes can escape NET-mediated killing via 3'-nucleotidase/nuclease activity [16]. PfTatD exhibits typical deoxyribonuclease activity and is likely utilized by *Plasmodium falciparum* to counteract NETs [48]. NETs induced by *Trypanosoma evansi* and *Trypanosoma brucei* could be hydrolyzed by native and recombinant TatD DNases [49]. Hookworm was the first helminth reported to use this strategy to evade capture by NETs [39]. Here, we also confirmed the presence of nucleases in *T. spiralis* ES that can be employed to degrade NETs as a conserved immune-evasion mechanism.

In addition to the direct degradation of NETs by nucleases secreted by some pathogens, many pathogens achieve immune escape by inhibiting the formation or release of NETs. Studies have shown that type 2 dengue virus (DENV-2) does not stimulate NETs production but rather inhibits NETs production in vitro; HIV inhibits ROS and NETs release by promoting IL-10 production [50]. Fungi also have their own unique countermeasures, and the surface hydrophobic protein RodA of *Aspergillus fumigatus* conidia is immune-inert, reducing the production of NETs and limiting the killing ability of NETs against spores [51]. *Schistosoma japonicum* inhibited NET formation in wild-type mice by upregulating host interleukin-10 (IL-10) expression [52]. Uptake of EVs derived from trophozoite-neutrophil coculture by neutrophils did not affect ROS production but instead caused a greater delay in the onset of NETs release and in their quantity [53]. ES antigens from *T. spiralis* inhibit NETs release, since neutrophils incubated with these antigens maintain a delobulated nucleus, without the release fiber structures indicative of NETs [19]. Kobpornchai et al. found that NETs activated with PMA were dramatically reduced when treated with serine protease inhibitor derived from *T. spiralis* (TsSERP) [54]. *T. spiralis* secretes calreticulin (TsCRT) binding to C1q also inhibited formation of NETs [55]. In this study, *T. spiralis* from three different developmental stages were cocultured with

neutrophils and macrophages, but NETs were produced only when neutrophils were cocultured with adults and macrophages were cocultured with ML and NBL. L Ríos-López et al. found that *T. spiralis* excretory–secretory antigens inhibit the release of extracellular traps from neutrophils [19]. Therefore, we suspect that NETs cannot be produced in the presence of ATA because the components in ES that inhibit the formation of NETs act more strongly than those that induce the release of NETs. *T. spiralis* completes the life cycle in the same host, and the immune cells encountered and the ES components secreted are different at different developmental stages, so it develops this complex immune escape strategy that can not only degrade ETs by nuclease but also inhibit the release of ETs. However, how these two strategies are balanced in the host remains to be further explored.

To identify the nuclease components in the ES, zymography and mass spectrometry were used, and nine DNase II family proteins (excluding miscellaneous proteins) were identified. In fact, compared with nucleases from other species, including *C. elegans*, the DNase II family proteins in *T. spiralis* are markedly expanded, with an estimated 125 genes in the genome [56]. A histidine residue that is surrounded by a highly conserved 5-mer DHSKW [22] has been proposed as the core catalytic center of most DNase II family members [23]. Of the 125 predicted genes and the 9 detected DNase II family proteins in *T. spiralis*, only plancitoxin-1 (*Ts*-Pt-1) possesses one predicted active site involved in DNA cleavage and is located in the C-terminus. During our identification of the protein, we once obtained an inaccurate sequence, which had no signal peptide [57]. Then, we corrected the sequence through NCBI ORF finder, obtained an accurate sequence with a signal peptide, and submitted it to GenBank (1095 bp, GenBank accession no. XM_003370715.1). In the present study, the DNase activity of one randomly selected protein that does not have the typical enzyme active centers and the recombinant *Ts*-Pt-1 protein (*rTs*-Pt-1) was examined, and the results showed that only *rTs*-Pt-1 had nuclease activity. The identification of the terminus of the enzymatic hydrolysates showed that *rTs*-Pt-1 belonged to DNase II, and its enzyme characteristics were found to be consistent with those of AD3 ES; thus, we speculated that the nuclease in the ES is plancitoxin-1. Unicellular pathogens usually secrete DNase I to degrade NETs [10], resulting in a strong cytokine storm that damages the host, while *T. spiralis*, a well-adapted nematode parasite that has evolved over thousands of years, uses DNase II to degrade NETs to escape the host immune response, greatly alleviating the inflammatory response of the host.

RNAi can reduce the expression of *Ts*-pt-1, weaken the evasion of the neutrophil immune response, and reduce

the number of worms. When anti-Ly6G was injected daily until 3 days after infection to deplete neutrophils, the depletion effect was maintained until the end of the intestinal phase, but because *Ts-pt-1* resisted not only the immune response of neutrophils but also the immune response of macrophages, eosinophils, mast cells, and other immune cells, only depletion of neutrophils did not restore the RNAi-mediated decline in the number of adult worms to normal levels. Moreover, the number of adult worms in the intestinal stage of *T. spiralis* infection determines the number of newborn larvae and muscle larvae. If the number of adult worms is reduced, the number of newborn larvae will be reduced, and the reduced newborn larvae will migrate to the muscle to form cysts; correspondingly, the number of muscle larvae will be reduced. Therefore, the number of adult worms in the intestinal stage and the number of muscle larvae will follow almost the same trend.

T. spiralis vaccines currently in development mainly target some proteins with high reactogenicity, but the key virulence factors of *T. spiralis* or the factors involved in immune evasion are still unclear, which limits the development of vaccines. In the present study, RNAi of *Ts-Pt-1* did not affect the viability of the worm or the ability to induce NETs, but the pathogenicity of the worm after interference decreased significantly, while the pathogenicity was restored after neutrophil depletion, indicating that *Ts-Pt-1* is a key virulence factor involved in defending the immune response of neutrophils in the process of *T. spiralis* infection. Moreover, the results from the immunoprotection assay indicated that *Ts-Pt-1* is worthy of further exploration as a potential vaccine candidate.

Conclusions

In conclusion, we discovered that neutrophils and macrophages could release ETs to capture and kill *T. spiralis*. However, plancitoxin-1, a DNase with biochemical features similar to those of the DNase II family, was found to be secreted by *T. spiralis* and can be exploited by the parasite to escape ET capture. The expression of this nuclease was found to be associated with parasite pathogenicity, and the deoxyribonuclease can thus be used as a potential candidate in *T. spiralis* vaccine development.

Methods

Animals, cell lines, and parasites

Female ICR mice (18–20 g), C57BL mice (aged 6–8 weeks), and Wistar rats (200 ± 20 g) were purchased from the Experimental Animal Centre of the College of Basic Medical Sciences, Jilin University (Changchun, China). All animals were maintained on standard rodent chow with water supplied ad libitum under a 12-h

light/12-h dark cycle during the experimental period. All experiments were conducted according to the regulations of the Administration of Affairs Concerning Experimental Animals in China. The procedure for animal experiments was approved by the Institutional Animal Care and Use Committee of Jilin University (permit no. 20170318).

The mouse mononuclear macrophage cell line J774A.1 was purchased from ATCC, and the cells were cultured in Dulbecco's modified Eagle's medium (DMEM; Corning, USA) supplemented with 10% fetal bovine serum (FBS; Gibco, USA) and 1% antibiotic–antimycotic solution (Corning, USA) at 37 °C with 5% CO₂.

The *T. spiralis* isolate (ISS534) was obtained from a naturally infected domestic pig in Henan Province in China and maintained in rats [58].

Preparation of excretory–secretory (ES) products of worms from three different developmental stages and crude extract of adult worms

T. spiralis-infected rat muscles were digested using an artificial digestion method to collect ML at 35 days postinfection (dpi) [59]. Adult worms were obtained from the rat intestine at 1, 3, and 6 dpi. Adult worms obtained at 6 dpi were cultured in RPMI-1640 (Gibco, USA) at 37 °C in 5% CO₂ for 18 h, and NBL were harvested [60]. All recovered worms were washed several times with normal saline containing 1% penicillin/streptomycin (Sigma–Aldrich, USA) to ensure that there was no residual bacteria or endotoxin. The secreted products of ML, adult worms, and NBL were prepared as previously described [59].

To exclude the leakage of nuclease proteins into ES due to worm death, we collected ES from 10,000 adult worms and crude extract from 30 live worms (the number was consistent with that of worms dead during culture of 10,000 adult worms) to compare the nuclease activities. The collection method of ES was consistent with the above, and the collection method of crude extract was as follows: after harvesting, washed adult worms were placed into a 1.5-ml centrifuge tube, and 50 µl of PBS containing PMSF (1 mM) was added to the tube. The tube was placed on ice, and the worms were fully ground with an electric tissue grinder. After centrifugation at 6000 × g and 4 °C for 15 min, the supernatant was collected and stored at –80 °C until use.

Neutrophil count

Tail vein blood was collected from infected C57BL mice (300 µl/mouse) at 0, 3, 7, 15, and 30 dpi. Approximately 100 µl of whole blood was added to an Eppendorf tube containing 10 µl of the anticoagulant ACD-B. Within 5 h, the blood was analyzed using a Hematology Coulter Ac.

T Diff. (Beckman Coulter) equipped with a veterinary card for the assessment of small animal blood.

A length of approximately 1 cm of duodenum approximately 1.5 cm from the pylorus of the mouse infected by *T. spiralis* was taken from ICR mice at 3 dpi, fixed with formalin, embedded in paraffin, and sliced with a microtome. Tissue slices were deparaffinized and subsequently treated in sodium citrate buffer (pH 6.0) with a 500-W microwave oven for 12 min to improve antigen retrieval. Then, the slices were treated with 3% hydrogen peroxide solution to block endogenous peroxidase activity. Nonspecific binding was blocked via incubation in PBS containing 5% normal goat serum for 30 min at room temperature. Then, the sections were incubated with an anti-Ly6G rabbit monoclonal antibody (1:2000 dilution; Abcam, UK) overnight at 4 °C. Subsequently, the slices were washed with PBS and incubated with a peroxidase-conjugated anti-rabbit secondary antibody (Beijing Biosynthesis Biotechnology Co. Ltd., China) for 30 min at room temperature, followed by 3,30-diaminobenzidine (DAB) and hematoxylin staining. Images were captured using an Olympus BX53 fluorescence microscope (Japan). The number of cells that were stained with the primary antibody was counted in all the photographs by three researchers who were blinded to the animal groupings, and the cell numbers were expressed as visible neutrophils per field.

Polymorphonuclear leukocyte (PMN) isolation and identification

PMNs were isolated from the bone marrow of C57BL/6 mice. Briefly, the bone marrow cells were rinsed from the femur and tibia, filtered, and then centrifuged at $400\times g$ for 10 min at room temperature (RT). The supernatant was discarded, and the pellet was suspended in diluent (cell concentration adjusted to 2×10^8 – 1×10^9 cells/ml) for use. The cell suspension was carefully layered on a separation solution (Solarbio, China) and centrifuged at $500\times g$ for 25 min at RT, and the milky white mononuclear cell layer was then isolated. Afterward, the PMNs were washed twice ($400\times g$, 10 min, RT), resuspended in RPMI-1640 medium, counted in a Neubauer hemocytometer chamber, and incubated at 37 °C in 5% CO₂ for at least 30 min before experimental use.

The isolated PMNs were incubated with FITC-CD11b (Abcam, UK) and PE-Ly6G (Abcam, UK) for 30 min at 4 °C in the dark to detect the cell purity. All washing steps were performed in PBS. The cells were detected with FACS (Beckman Coulter, USA), and the data were analyzed with FlowJo software (TreeStar Software, USA). The nuclear morphology of PMNs was observed under a fluorescence microscope after staining with Hoechst

33342 (1:30,000; Sigma–Aldrich, USA) for 10 min at room temperature.

NET visualization by immunofluorescence analysis

PMNs (2×10^5 /well) were seeded on poly-L-lysine-treated glass coverslips placed in 24-well plates or on bottom chambers in transwell plates in serum-free RPMI-1640 medium without phenol red (Gibco, USA) and supplemented with 1% penicillin/streptomycin (Gibco, USA) (this medium was used in all experiments related to NETs in this study). After 1 h of stability, aurintricarboxylic acid (ATA) (Sigma–Aldrich, USA) at a final concentration of 25 μM was added or not to the medium, and the cells were then cocultured with adult worms obtained at 3 dpi (AD3) (live or heat-killed at 56 °C for 30 min, 50 worms/well) for 3 h at 37 °C in 5% CO₂. Dead worms do not move and are in a stretching state, and the analysis of worm killing was performed by blinded researchers. For transwell plates, AD3 were added to the top well. Subsequently, the samples were fixed in 4% paraformaldehyde (Merck, Germany) and maintained at 4 °C until further use. The NET structures were visualized by staining extracellular DNA with SYTOX Green (5 μM, 15 min; Invitrogen, USA). For the detection of histones, myeloperoxidase (MPO), and neutrophil elastase (NE) on NET structures, the following antibodies were used: anti-histone H3 (ab61251, 1:100; Abcam, UK), anti-MPO (ab9535, 1:100; Abcam, UK), and anti-NE (ab21595, 1:100; Abcam, UK). Briefly, the samples were washed three times in PBS, blocked with 5% bovine serum albumin (Sigma–Aldrich, USA) at RT for 2 h and incubated in antibody solutions overnight at 4 °C. The samples were then washed three times with PBS, incubated in secondary antibody solutions (Alexa Fluor 555 goat anti-rabbit IgG, 1: 1,000; Abcam, UK) for 2 h at RT, washed three times in PBS, stained with SYTOX Green (5 μM; Invitrogen, USA), and Hoechst 33,342 (1: 30,000; Sigma–Aldrich, USA) for 15 min at RT and mounted in antifade buffer (Thermo Fisher Scientific, USA). Visualization was achieved using an inverted Olympus IX81 fluorescence microscope equipped with a digital camera (Olympus, Japan).

To acquire videos, PMNs (2×10^5 /dish) were cocultured with AD3 (50 worms/dish) in laser confocal microscopy petri dishes under the same culture conditions. After 3 h of cocultivation, SYTOX Green and Hoechst 33,342 were added to the medium for 15 min, and images were acquired with a laser scanning confocal microscope (Olympus, Japan).

Scanning electron microscopy (SEM)

J774A.1 cells (1×10^4 /well) were cocultured with ML (100 larvae/well) or NBL (400 larvae/well) on poly-L-lysine

(Sigma–Aldrich, USA)-precoated coverslips at 37 °C for 3 h with ATA at a final concentration of 25 μM in the culture medium. After incubation, the samples were fixed in 2.5% glutaraldehyde (Merck, Germany) overnight at 4 °C, postfixed in 1% osmium tetroxide (Merck, Germany), washed in distilled water, dehydrated, critical point dried by CO_2 treatment, and sprayed with gold. The samples were then examined with a scanning electron microscope (Hitachi S-3400 N, Japan).

Quantification of extracellular DNA release from PMNs

PMNs (2×10^5 , $n=3$ in duplicate) were seeded in 24-well plates and cocultured with AD3 worms (10, 20, 40, or 80 worms/well) for 0.5, 1, 2, 4, and 5 h, and the cell culture supernatant was then collected. The fluorescence value of extracellular DNA in the supernatant released from PMNs was measured with PicoGreen (Yeasen, China). Briefly, 100 μl of supernatant from each sample was placed in a 96-well plate, and 100 μl of PicoGreen detection reagent was then added to each well. The samples were incubated for 2–5 min at RT and protected from light. The fluorescence values of each well were detected in a fluorescence microplate reader (Bio-Tek, USA) with excitation/emission wavelengths of 480 nm/520 nm.

Identification of the source of the DNA scaffold

PMNs (4×10^5 cells/well) were seeded in a 24-well cell culture plate. Approximately 50 AD3 worms were added to each well and cocultured with the PMNs for 3 h. After cocultivation, the culture medium containing released DNA was aspirated and centrifuged at $1200 \times g$ for 5 min, and the supernatant was collected to serve as a PCR template. The culture supernatant of PMNs without any stimulation was used as a negative template. The cells of the negative control group were collected, and the total DNA of the cells extracted with DNAzol reagent (Invitrogen, USA) was used as a positive template. Primers for the detection of mouse nuclear genome genes (Rho, GAPDH, Actb, and Fas) and mitochondrial genome genes (Nd1, Cox1, Atp6, and Cyb) were designed as shown in Additional file 7: Table 1. PCR was carried out in a 25- μl reaction system for 30 cycles of 94 °C for 30 s, 58 °C for 30 s, and 72 °C for 30 s. The PCR products were run on 1% agarose gels.

Analysis of ET- or ADCP-mediated worm killing

PMNs (2×10^5 /well) were seeded in 24-well plates and cocultured with AD3 worms (50 worms/well) for 18 h at 37 °C in 5% CO_2 . The reference samples were prepared with an equal number of nonexposed AD3. Worm survival was determined microscopically based on the presence or absence of motility and the morphology of worms (dead worms were in a stretching state). The method

used for the cocultivation of J774A.1 and ML or NBL was the same as that described above, with the exception that mouse anti-*T. spiralis* serum was added to the medium to observe the worm-killing effect.

Detection of nuclease activity of AD3 ES

PMNs (1×10^6 cells) were seeded in a laser confocal culture dish and incubated with 100 nM phorbol-12-myristate-13-acetate (PMA; Sigma–Aldrich, USA) for 3 h to produce NETs. Hoechst 33,342 and SYTOX Green were added to the dish for fluorescence staining, and NETs were observed under a laser confocal microscope. The concentrated AD3 ES product was then added to the dish at a final concentration of 1 $\mu\text{g}/\mu\text{l}$ to determine whether it would degrade the DNA scaffold structure of NETs, and the samples were photographed at different time points.

To detect the optimal pH value of the nuclease in AD3 ES and to determine whether the nuclease activity depended on divalent metal ions, agarose gel electrophoresis and spectrophotometry were performed. For agarose gel electrophoresis, the 20- μl reaction system consisted of 10 μl of reaction buffer with different pH values (pH 4–10), 0.2 μg of λDNA (Sangon, China), 5 μg of AD3 ES, the absence or presence of 5 mM $\text{Ca}^{2+}/\text{Mg}^{2+}$ or 1 mM EDTA, and sufficient ddH₂O to obtain a total volume of 20 μl . The mixture was vortexed, briefly centrifuged and placed in a 37 °C water bath for 1 h. The reaction product was then loaded onto a 1% agarose gel and electrophoresed to observe the degradation of the substrate DNA. For spectrophotometry, the above-described 20- μl system was expanded to 100 μl . After the reaction was completed, the samples were placed on ice, and 100 μl of precooled 10% perchloric acid solution was added to terminate the reaction. The samples were then centrifuged at $13,000 \times g$ for 10 min at RT, the supernatant was transferred to a 96-well plate, and the absorbance at 260 nm was measured with a microplate reader (Tecan Infinite 200, Switzerland). A line chart was obtained by plotting the pH value on the abscissa and the absorbance on the ordinate.

SDS–PAGE zymography and mass spectrometry

A modified method described by Detwiler and Macintyre was used for SDS–PAGE zymography activity gels to determine the molecular weight of the nuclease in AD3 ES [61]. Briefly, an SDS–PAGE gel containing 50 $\mu\text{g}/\text{ml}$ salmon sperm DNA (Sigma–Aldrich, USA) in the separation gel (12%) but not in the concentration gel (4%) was prepared. AD3 ES was incubated in loading buffer without β -mercaptoethanol at 37 °C for 15 min and electrophoresed at 4 °C. After electrophoresis, the gels were shaken gently in 2.5% Triton X-100 (Sigma–Aldrich,

USA) at 4 °C for 30 min with 4 changes of buffer and subsequently rinsed in 50 mM sodium acetate (pH 5.0) reaction buffer. For the DNase reaction, the gels were incubated at 37 °C for 36 h in reaction buffer. The gels were stained with ethidium bromide, visualized with UV light, and subsequently stained with Coomassie brilliant blue.

The DNase bands were excised from SDS–PAGE zymography gels and stored in ultrapure water. LC–MS/MS was performed by ProtTech, Inc. (Phoenixville). Briefly, the sample was cleaned by washing with water and digested in-gel with trypsin in digestion buffer (100 mM ammonium bicarbonate, pH 8.5). The peptides were extracted with acetonitrile, completely dried, redissolved, and analyzed by NanoLC–ESI–MS/MS. The MS data were used to search against the nonredundant protein database (NR database, NCBI) using the ProTech ProtQuest software suite.

Cloning, expression, and enzyme characterization of DNase II-8, P43, T314, and Ts-Pt-1

Total RNA from ML was extracted using a TRIzol RNA extraction kit (Invitrogen, USA) and transcribed into first-strand cDNA with a SuperScript II RT cDNA synthesis kit (Invitrogen, USA) according to the manufacturer's instructions. The primers (Additional file 7: Table 2) were used to amplify the DNase II-8, P43, T314, and Ts-Pt-1 genes from cDNA, and the target genes were then cloned and inserted into the pcDNA 3.1/His A vector (Invitrogen, USA). Recombinant proteins were expressed after the plasmids were transfected into CHO cells with Lipofectamine 2000 (Invitrogen, USA), and the proteins were purified by affinity chromatography using a His-Trap purification kit (GE, USA) according to the manufacturer's instructions.

The nuclease activity of recombinant proteins was measured using the single radial enzyme-diffusion (SRED) method as previously described [62]. Briefly, 10 µl of recombinant proteins (0.1 µg/µl) was dispensed into a circular well in an agarose gel layer in which DNA and ethidium bromide were uniformly distributed. A circular dark zone formed as the enzyme diffused radially from the well into the gel and digested substrate DNA. The methods used to analyze the optimal pH of *rTs-Pt-1* and to detect the effect of metal ions on nuclease activity were the same as those used for AD3 ES.

To further confirm the enzymatic properties of *rTs-Pt-1*, phosphodiesterase I or phosphodiesterase II was added to 5 µg of enzymatic hydrolysates to continue the degradation reaction. The reaction buffers of phosphodiesterase I and phosphodiesterase II were 50 mM Tris–HCl (pH 8.8) with 10 mM MgCl₂ and 50 mM sodium phosphate (pH 6.5) with 10 mM MgCl₂, respectively.

After 30 min of incubation, perchloric acid was added to terminate the reaction, and the absorbance of the supernatant at 260 nm was measured after centrifugation. An increase in absorbance compared with that of the blank group indicated that the degradation reaction had occurred. Cleavage by phosphodiesterase II but not by phosphodiesterase I is a characteristic of DNase II enzymatic hydrolysates.

Real-time quantitative PCR (qPCR) analysis of Ts-Pt-1 gene transcription

cDNA from adult worms, NBL, and ML (Normal or siRNA-interfered) was obtained using the above-described methods. The transcription levels of *Ts-Pt-1* were evaluated with a forward primer (5'-GAATAATAC TGCAACTGGAAT-3') and reverse primer (5'-TTT AGGAATGCTGTGAATTAG-3'). The target gene was normalized to GAPDH (gene ID: AF452239) amplified with a forward primer (5'-GCTCCTATGTTGGTT ATGGG-3') and reverse primer (5'-TTTGGGTTGCCG TTGTAG-3'). qPCR was performed on an ABI Prism 7500 sequence detection instrument (Applied Biosystems, USA). The relative expression of *Ts-Pt-1* at different developmental stages was determined using the 2^{−ΔΔCT} method. Three independent experiments were performed.

Western blot analysis of rTs-Pt-1

The *rTs-Pt-1* were run on an SDS–PAGE gel and analyzed by Western blot. Briefly, the protein was electrophoresed on 12% SDS–PAGE gels and then transferred to 0.2-mm nitrocellulose membranes using the semi-dry blotting system (Bio-Rad, CA, USA). The membranes were cut into strips, blocked with 5% (W/V) skim milk in Tris-buffered saline with 0.05% Tween 20 (TBST), and incubated with serum (1:400) collected from *T. spiralis*-infected pigs (10,000 ML/pig) and ICR mice (500 ML/mouse) in our laboratory at 37 °C for 2 h. In addition, normal pig and mouse serum were used as negative controls. HRP-labeled goat anti-pig IgG (1:400) (Solarbio, China) or HRP-labeled goat anti-mouse IgG (1: 6000) (Abcam, UK) was used as the secondary antibody. After washing, the strips were treated using an enhanced chemiluminescence (ECL) kit (Thermo Fisher, USA).

The effect of antisera on the nuclease activity of plancitoxin-1

Antisera against *rTs-Pt-1* were produced in a rabbit injected subcutaneously with approximately 500 µg of purified *rTs-Pt-1* mixed with complete Freund's adjuvant (FCA, Sigma, USA). Three additional booster injections containing 250 µg of *rTs-Pt-1* mixed with incomplete Freund's adjuvant (IFA, Sigma, USA) were injected

intradermally at 2-week intervals. Antibodies from blood serum were affinity purified using Protein A Sefinose (Sangon, China) according to the manufacturer's instructions. The affinity-purified antibodies were added to the nuclease reaction system to detect their effect on the nuclease activity of plancitoxin-1.

Immunolocalization

Slices of *T. spiralis* adults were prepared as described above. Whole worms and duodenum sections were immersed in fixative solution (3.7% formaldehyde for 10 min, cold 100% MeOH for 5 min) and permeabilized by incubation in PBS containing 1% Triton X-100 for 5 min. All the samples were blocked with 3% BSA in PBST (PBS containing 0.1% Triton X-100) and then incubated with a rabbit anti-r*Ts*-Pt-1 polyclonal antibody at 4 °C overnight. Following three washes in PBST, the samples were incubated with an Alexa Fluor 594-labeled goat anti-rabbit IgG fluorescent antibody (Invitrogen, USA) at room temperature for 1 h. The samples were washed three times in PBST, stained with Hoechst 33,342 (Invitrogen, USA) for 10 min, washed three additional times in PBST, mounted with 70% glycerol on slides, and observed under a fluorescence microscope (Olympus, Japan).

RNAi

Full-length mRNA encoding *Ts*-Pt-1 was utilized to design siRNA sequences using siDirect version 2.0 [63]. The *Ts*-Pt-1-specific siRNA oligos (Stealth™ RNAi duplexes) used in this work were chemically synthesized by Sangon (Shanghai, China). The sequences of the three specific siRNAs and control siRNAs used in this study are listed in Additional file 7: Table 3. The same control FAM-labeled siRNA (Sango, China) was used to evaluate the transfection efficiency. Incubation methods were used to deliver specific or control siRNA into the larvae. A total of 5000 ML were suspended in a final volume of 500 µl of RPMI 1640 culture medium (Gibco, USA) supplemented with 100 U/ml penicillin and 100 mg/ml streptomycin for incubation. Control siRNA or specific siRNA was incubated with 2 ml of lipofectamine 2000 (Invitrogen, USA) for 20 min before being added to the larvae at a final concentration of 2 µM. The incubation was continued at 37 °C and 5% CO₂ for 24 h. FAM-labeled control siRNA was used to visualize the uptake of siRNA.

After 24 h of treatment with siRNA, qPCR and Western blotting were performed to evaluate target gene expression. The qPCR protocol was the same as that described above. For Western blotting, rabbit anti-r*Ts*-Pt-1 serum (1: 1000) was used as the primary antibody, and a rabbit antibody against GAPDH (1: 1000) (Proteintech, USA) was used to detect GAPDH expression as a quantitative

protein control. HRP-conjugated goat anti-rabbit IgG (1:5000) was used as the secondary antibody.

Nuclease activity detection of ES obtained from AD3 treated with siRNA

Each ICR mouse was gavaged with 1200 larvae treated with siRNA 290, and adults were collected after 3 days of infection. The ES of AD3 was collected according to the above-described method, and the above-described agarose gel electrophoresis and single radial enzyme-diffusion (SRED) methods were used to detect the change in the nuclease activity intensity of ES compared with the control to verify that the nuclease in ES was plancitoxin-1. Twenty-four mice were divided into four groups: two groups of mice were wild mice, and the other two groups were neutrophil-depleted mice. Wild-type mice and neutrophil-depleted mice were gavaged with 300 normal ML and 300 ML treated with siRNA 290, respectively. For neutrophil-depleted mice, anti-Ly6G mAb (Abcam, UK) (0.5 mg/mouse) was administered intraperitoneally once a day from the day before infection to 3 days after infection. Cellular depletion efficiency was evaluated by imaging the infected intestine. Adult worms and muscle larvae were then collected at 7 dpi and 35 dpi, respectively, and the datasets were compared.

Immunoprotective analysis of r*Ts*-pt-1

For the first immunization, 50 µg/mouse (ICR, female, aged 6 to 8 weeks) r*Ts*-pt-1 emulsified with complete Freund's adjuvant was intramuscularly injected, and two immunizations with 50 µg recombinant protein emulsified with incomplete Freund's adjuvant were then administered at 2-week intervals. The mice in the control group were injected with Freund's adjuvant only. Seven days after the three immunizations, the mice were infected with 300 ML. Adult worms and muscle larvae were collected at 7 dpi and 35 dpi, respectively. The number of muscle larvae per gram of muscle (LPG) and the worm reduction rate were evaluated in comparison with those of the control group.

Statistical analysis

All results are expressed as the means ± SDs. The statistical analyses were performed using GraphPad Prism 8. One-way analysis of variance (ANOVA) or Student's *t* test was used to compare significant differences under different conditions. The *p* values are expressed as **p* < 0.05, ***p* < 0.01, ****p* < 0.001, *****p* < 0.0001 (ns, no significant difference, *P* > 0.05).

Abbreviations

ETs	Extracellular traps
NETs	Neutrophil extracellular traps
METs	Macrophage extracellular traps

ML	Muscle larvae
NBL	Newborn larvae
AD3	Adult worms obtained at 3 days post infection
ES	Excretory/secretory products
PMNs	Polymorphonuclear leukocytes
ATA	Aurintricarboxylic acid
ADCP	Antibody-dependent cellular phagocytosis
PMA	Phorbol-12-myristate-13-acetate
dpi	Days postinfection
PMSF	Phenylmethanesulfonyl fluoride
H3	Histone 3
MPO	Myeloperoxidase
NE	Neutrophil elastase
RT	Room temperature
SEM	Scanning electron microscopy

Supplementary Information

The online version contains supplementary material available at <https://doi.org/10.1186/s12915-024-01958-2>.

Additional file 1: Figs. S1–S10.

Additional file 2: Video S1 NETs formation induced by adult worms with ATA in culture medium.

Additional file 3: Video S2 METs formation induced by NBL with ATA in culture medium.

Additional file 4: Video S3 NETs limit the movement area of adult worms.

Additional file 5: Video S4 Adult worms can move freely over a large range without NETs formation.

Additional file 6: Video S5 The ADCP effect of macrophages has a killing effect on NBL.

Additional file 7: Table 2.

Acknowledgements

We thank Xinrui Wang and Yuanyuan Zhang from the Instrument Center of the Institute of Zoonoses, Jilin University, China, for assisting us with image acquisition. We thank Dr. Pan Liu for his help in the smooth conduct of the experiments.

Authors' contributions

J.D., N.X., X.L., and M.L. designed the study, analyzed and interpreted the data, and prepared the manuscript. J.D., J.W., N.X., and Y.H. performed the experiments and interpreted the data. J.D. and Y.H. performed the bioinformatic analysis, and X.W. interpreted the findings. All the authors reviewed, commented on, and approved the manuscript.

Funding

This work was supported by the National Key Research and Development Program of China (2021YFC2600202) and the National Natural Science Foundation of China (NSFC32230104, 32202835), Science and Technology talents and platform plan of Yunnan province (Academician and Expert Workstation, 202305AF150167), and the Fundamental Research Funds for the Central Universities.

Availability of data and materials

All data generated or analyzed during this study are included in this published article, and its supplementary information files. The mass spectrometry raw data that support the findings of this study could be accessed in iProX (<https://www.iprox.org/>) with Project ID PXD048428 (<https://proteomecentral.proteomexchange.org/cgi/GetDataset?ID=PXD048428>). The other data supporting the findings of this study are available from the corresponding authors upon request.

Declarations

Ethics approval and consent to participate

All experiments were conducted according to the regulations of the Administration of Affairs Concerning Experimental Animals in China. The procedure for animal experiments was approved by the Institutional Animal Care and Use Committee of Jilin University (Permit No. 20170318).

Consent for publication

Not applicable.

Competing interests

The authors declare that they have no competing interests.

Received: 8 March 2023 Accepted: 15 July 2024

Published online: 29 July 2024

References

- Bintsis T. Foodborne pathogens. *AIMS Microbiol.* 2017;3(3):529–63.
- Li C, Bai X, Liu X, Zhang Y, Liu L, Zhang L, Xu F, Yang Y, Liu M. Disruption of epithelial barrier of Caco-2 Cell monolayers by excretory secretory products of *Trichinella spiralis* might be related to serine protease. *Front Microbiol.* 2021;12:634185.
- Xu J, Liu RD, Bai SJ, Hao HN, Yue WW, Xu YXY, Long SR, Cui J, Wang ZQ. Molecular characterization of a *Trichinella spiralis* aspartic protease and its facilitation role in larval invasion of host intestinal epithelial cells. *Plos Negl Trop Dis.* 2020;14(4):e0008269.
- Bai Y, Ma KN, Sun XY, Dan Liu R, Long SR, Jiang P, Wang ZQ, Cui J. Molecular characterization of a novel cathepsin L from *Trichinella spiralis* and its participation in invasion, development and reproduction. *Acta Trop.* 2021;224:106112.
- Yi N, Yu P, Wu L, Liu Z, Guan J, Liu C, Liu M, Lu Y. RNAi-mediated silencing of *Trichinella spiralis* serpin-type serine protease inhibitors results in a reduction in larval infectivity. *Vet Res.* 2020;51(1):139.
- Xu N, Bai X, Liu Y, Yang Y, Tang B, Shi HN, Vallee I, Boireau P, Liu X, Liu M. The anti-inflammatory immune response in early *Trichinella spiralis* intestinal infection depends on serine protease inhibitor-mediated alternative activation of macrophages. *J Immunol (Baltimore, Md : 1950).* 2021;206(5):963–77.
- Mak CH, Ko RC. Characterization of endonuclease activity from excretory/secretory products of a parasitic nematode *Trichinella spiralis*. *Eur J Biochem.* 1999;260(2):477–81.
- Brinkmann V, Reichard U, Goosmann C, Fauler B, Uhlemann Y, Weiss DS, Weinrauch Y, Zychlinsky A. Neutrophil extracellular traps kill bacteria. *Science (New York, NY).* 2004;303(5663):1532–5.
- Chow OA, von Köckritz-Blickwede M, Bright AT, Hensler ME, Zinkernagel AS, Cogen AL, Gallo RL, Monestier M, Wang Y, Glass CK, et al. Statins enhance formation of phagocyte extracellular traps. *Cell Host Microbe.* 2010;8(5):445–54.
- Beiter K, Wartha F, Albiger B, Normark S, Zychlinsky A, Henriques-Normark B. An endonuclease allows *Streptococcus pneumoniae* to escape from neutrophil extracellular traps. *Curr Biol : CB.* 2006;16(4):401–7.
- Seper A, Hosseinzadeh A, Gorkiewicz G, Lichtenegger S, Roier S, Leitner DR, Röhm M, Grutsch A, Reidl J, Urban CF, et al. *Vibrio cholerae* evades neutrophil extracellular traps by the activity of two extracellular nucleases. *Plos Pathog.* 2013;9(9):e1003614.
- Berends ET, Horswill AR, Haste NM, Monestier M, Nizet V, von Köckritz-Blickwede M. Nuclease expression by *Staphylococcus aureus* facilitates escape from neutrophil extracellular traps. *J Innate Immun.* 2010;2(6):576–86.
- Buchanan JT, Simpson AJ, Aziz RK, Liu GY, Kristian SA, Kotb M, Feramisco J, Nizet V. DNase expression allows the pathogen group a *Streptococcus* to escape killing in neutrophil extracellular traps. *Curr Biol : CB.* 2006;16(4):396–400.
- Morita C, Sumioka R, Nakata M, Okahashi N, Wada S, Yamashiro T, Hayashi M, Hamada S, Sumitomo T, Kawabata S. Cell wall-anchored nuclease of *Streptococcus sanguinis* contributes to escape from

- neutrophil extracellular trap-mediated bacteriocidal activity. Plos One. 2014;9(8):e103125.
15. Loureiro A, Pais C, Sampaio P. Relevance of macrophage extracellular traps in *C. albicans* killing. Front Immunol. 2019;10:2767.
 16. Guimarães-Costa AB, DeSouza-Vieira TS, Paletta-Silva R, Freitas-Mesquita AL, Meyer-Fernandes JR, Saraiva EM. 3'-nucleotidase/nuclease activity allows Leishmania parasites to escape killing by neutrophil extracellular traps. Infect Immun. 2014;82(4):1732–40.
 17. Jasmer DP, Kwak D. Fusion and differentiation of murine C2C12 skeletal muscle cells that express *Trichinella spiralis* p43 protein. Exp Parasitol. 2006;112(2):67–75.
 18. Macanovic M, Lachmann PJ. Measurement of deoxyribonuclease I (DNase) in the serum and urine of systemic lupus erythematosus (SLE)-prone NZB/NZW mice by a new radial enzyme diffusion assay. Clin Exp Immunol. 1997;108(2):220–6.
 19. Rios-Lopez AL, Hernández-Bello R, González GM, Sánchez-González A. *Trichinella spiralis* excretory-secretory antigens selectively inhibit the release of extracellular traps from neutrophils without affecting their additional antimicrobial functions. Cell Immunol. 2022;382:104630.
 20. Liu P, Wu X, Liao C, Liu X, Du J, Shi H, Wang X, Bai X, Peng P, Yu L, et al. *Escherichia coli* and *Candida albicans* induced macrophage extracellular trap-like structures with limited microbicidal activity. Plos One. 2014;9(2):e90042.
 21. Kaplan BS, Uni S, Aikawa M, Mahmoud AA. Effector mechanism of host resistance in murine giardiasis: specific IgG and IgA cell-mediated toxicity. J Immunol (Baltimore, Md : 1950). 1985;134(3):1975–81.
 22. Krieser RJ, MacLea KS, Park JP, Eastman A. The cloning, genomic structure, localization, and expression of human deoxyribonuclease IIbeta. Gene. 2001;269(1–2):205–16.
 23. Schäfer P, Cymerman IA, Bujnicki JM, Meiss G. Human lysosomal DNase IIalpha contains two requisite PLD-signature (HxK) motifs: evidence for a pseudodimeric structure of the active enzyme species. Protein Sci : Public Protein Soc. 2007;16(1):82–91.
 24. Choo KH, Jennings IG, Cotton RG. Comparative studies of four monoclonal antibodies to phenylalanine hydroxylase exhibiting different properties with respect to substrate-dependence, species-specificity and a range of effects on enzyme activity. Biochem J. 1981;199(3):527–35.
 25. Ding J, Liu X, Bai X, Wang Y, Li J, Wang C, Li S, Liu M, Wang X. *Trichinella spiralis*: inflammation modulator. J Helminthol. 2020;94: e193.
 26. Delgado-Rizo V, Martínez-Guzmán MA, Iñiguez-Gutierrez L, García-Orozco A, Alvarado-Navarro A, Fafutis-Morris M. Neutrophil extracellular traps and its implications in inflammation: an overview. Front Immunol. 2017;8:81.
 27. Daniel C, Leppkes M, Muñoz LE, Schley G, Schett G, Herrmann M. Extracellular DNA traps in inflammation, injury and healing. Nat Rev Nephrol. 2019;15(9):559–75.
 28. Baker VS, Imade GE, Molta NB, Tawde P, Pam SD, Obadofin MO, Sagay SA, Egah DZ, Iya D, Afolabi BB, et al. Cytokine-associated neutrophil extracellular traps and antinuclear antibodies in *Plasmodium falciparum* infected children under six years of age. Malar J. 2008;7:41.
 29. Waisberg M, Molina-Cruz A, Mizurini DM, Gera N, Sousa BC, Ma D, Leal AC, Gomes T, Kotsyfakis M, Ribeiro JM, et al. *Plasmodium falciparum* infection induces expression of a mosquito salivary protein (Agaphelin) that targets neutrophil function and inhibits thrombosis without impairing hemostasis. Plos Pathog. 2014;10(9):e1004338.
 30. Abi Abdallah DS, Lin C, Ball CJ, King MR, Duhamel GE, Denkers EY. *Toxoplasma gondii* triggers release of human and mouse neutrophil extracellular traps. Infect Immun. 2012;80(2):768–77.
 31. Guimarães-Costa AB, Nascimento MT, Froment GS, Soares RP, Morgado FN, Conceição-Silva F, Saraiva EM. *Leishmania amazonensis* promastigotes induce and are killed by neutrophil extracellular traps. Proc Natl Acad Sci USA. 2009;106(16):6748–53.
 32. Sousa-Rocha D, Thomaz-Tobias M, Diniz LF, Souza PS, Pinge-Filho P, Toledo KA. *Trypanosoma cruzi* and its soluble antigens induce NET release by stimulating Toll-like receptors. Plos One. 2015;10(10):e0139569.
 33. Behrendt JH, Ruiz A, Zahner H, Taubert A, Hermosilla C. Neutrophil extracellular trap formation as innate immune reactions against the apicomplexan parasite *Eimeria bovis*. Vet Immunol Immunopathol. 2010;133(1):1–8.
 34. Wei Z, Hermosilla C, Taubert A, He X, Wang X, Gong P, Li J, Yang Z, Zhang X. Canine Neutrophil extracellular traps release induced by the apicomplexan parasite *Neospora caninum* in vitro. Front Immunol. 2016;7:436.
 35. Bonne-Année S, Kerepesi LA, Hess JA, Wesolowski J, Paumet F, Lok JB, Nolan TJ, Abraham D. Extracellular traps are associated with human and mouse neutrophil and macrophage mediated killing of larval *Strongyloides stercoralis*. Microbes Infect. 2014;16(6):502–11.
 36. Chuah C, Jones MK, Burke ML, McManus DP, Owen HC, Gobert GN. Defining a pro-inflammatory neutrophil phenotype in response to schistosome eggs. Cell Microbiol. 2014;16(11):1666–77.
 37. Muñoz-Caro T, Rubio RM, Silva LM, Magdowski G, Gärtner U, McNeilly TN, Taubert A, Hermosilla C. Leucocyte-derived extracellular trap formation significantly contributes to *Haemonchus contortus* larval entrapment. Parasit Vectors. 2015;8:607.
 38. Muñoz-Caro T, Conejeros I, Zhou E, Pikhovych A, Gärtner U, Hermosilla C, Kulke D, Taubert A. *Dirofilaria immitis* microfilariae and third-stage larvae induce canine NETosis resulting in different types of neutrophil extracellular traps. Front Immunol. 2018;9:968.
 39. Bouchery T, Moyat M, Sotillo J, Silverstein S, Volpe B, Coakley G, Tsourouktsoglou TD, Becker L, Shah K, Kulagin M, et al. Hookworms evade host immunity by secreting a deoxyribonuclease to degrade neutrophil extracellular traps. Cell Host Microbe. 2020;27(2):277–289.e276.
 40. Ehrens A, Lenz B, Neumann AL, Giarrizzo S, Reichwald JJ, Frohberger SJ, Stammering W, Buerfernt BC, Fercoq F, Martin C, et al. Microfilariae trigger eosinophil extracellular DNA traps in a dectin-1-dependent manner. Cell Rep. 2021;34(2):108621.
 41. Fuchs TA, Abed U, Goosmann C, Hurwitz R, Schulze I, Wahn V, Weinrauch Y, Brinkmann V, Zychlinsky A. Novel cell death program leads to neutrophil extracellular traps. J Cell Biol. 2007;176(2):231–41.
 42. von Köckritz-Blickwede M, Goldmann O, Thulin P, Heinemann K, Norrby-Teglund A, Rohde M, Medina E. Phagocytosis-independent antimicrobial activity of mast cells by means of extracellular trap formation. Blood. 2008;111(6):3070–80.
 43. Yousefi S, Gold JA, Andina N, Lee JJ, Kelly AM, Kozłowski E, Schmid I, Straumann A, Reichenbach J, Gleich GJ, et al. Catapult-like release of mitochondrial DNA by eosinophils contributes to antibacterial defense. Nat Med. 2008;14(9):949–53.
 44. Yousefi S, Mihalache C, Kozłowski E, Schmid I, Simon HU. Viable neutrophils release mitochondrial DNA to form neutrophil extracellular traps. Cell Death Differ. 2009;16(11):1438–44.
 45. Storișteanu DM, Pocock JM, Cowburn AS, Juss JK, Nadesalingam A, Nizet V, Chilvers ER. Evasion of neutrophil extracellular traps by respiratory pathogens. Am J Respir Cell Mol Biol. 2017;56(4):423–31.
 46. Medina E. Neutrophil extracellular traps: a strategic tactic to defeat pathogens with potential consequences for the host. J Innate Immun. 2009;1(3):176–80.
 47. Zhang X, Zhao S, Sun L, Li W, Wei Q, Ashman RB, Hu Y. Different virulence of *Candida albicans* is attributed to the ability of escape from neutrophil extracellular traps by secretion of DNase. Am J Transl Res. 2017;9(1):50–62.
 48. Chang Z, Jiang N, Zhang Y, Lu H, Yin J, Wahlgren M, Cheng X, Cao Y, Chen Q. The TatD-like DNase of *Plasmodium* is a virulence factor and a potential malaria vaccine candidate. Nat Commun. 2016;7:11537.
 49. Zhang K, Jiang N, Chen H, Zhang N, Sang X, Feng Y, Chen R, Chen Q. TatD DNases of *African trypanosomes* confer resistance to host neutrophil extracellular traps. Sci China Life Sci. 2021;64(4):621–32.
 50. Saitoh T, Komano J, Saitoh Y, Misawa T, Takahama M, Kozaki T, Uehata T, Iwasaki H, Omori H, Yamaoka S, et al. Neutrophil extracellular traps mediate a host defense response to human immunodeficiency virus-1. Cell Host Microbe. 2012;12(1):109–16.
 51. Bruns S, Kniemeyer O, Hasenberg M, Aimaniananda V, Nietzsche S, Thywissen A, Jeron A, Latgé JP, Brakhage AA, Gunzer M. Production of extracellular traps against *Aspergillus fumigatus* in vitro and in infected lung tissue is dependent on invading neutrophils and influenced by hydrophobin RodA. Plos Pathog. 2010;6(4):e1000873.
 52. Wang L, Zhu Z, Liao Y, Zhang L, Yu Z, Yang R, Wu J, Wu Z, Sun X. Host liver-derived extracellular vesicles deliver miR-142a-3p induces neutrophil extracellular traps via targeting WASL to block the development of *Schistosoma japonicum*. Mol Ther : J Am Soc Gene Ther. 2022;30(5):2092–107.
 53. Díaz-Godínez C, Rios-Valencia DG, García-Aguirre S, Martínez-Calvillo S, Carrero JC. Immunomodulatory effect of extracellular vesicles from *Entamoeba histolytica* trophozoites: regulation of NETs and respiratory burst during confrontation with human neutrophils. Front Cell Infect Microbiol. 2022;12:1018314.

54. Kobpornchai P, Reamtong O, Phuphisut O, Malaitong P, Adisakwattana P. Serine protease inhibitor derived from *Trichinella spiralis* (TsSERP) inhibits neutrophil elastase and impairs human neutrophil functions. *Front Cell Infect Microbiol.* 2022;12:919835.
55. Shao S, Hao C, Zhan B, Zhuang Q, Zhao L, Chen Y, Huang J, Zhu X. *Trichinella spiralis* Calreticulin S-domain binds to human complement C1q to interfere with C1q-mediated immune functions. *Front Immunol.* 2020;11:572326.
56. Mitreva M, Jasmer DP, Zarlenga DS, Wang Z, Abubucker S, Martin J, Taylor CM, Yin Y, Fulton L, Minx P, et al. The draft genome of the parasitic nematode *Trichinella spiralis*. *Nat Genet.* 2011;43(3):228–35.
57. Liao C, Liu M, Bai X, Liu P, Wang X, Li T, Tang B, Gao H, Sun Q, Liu X, et al. Characterisation of a plancitoxin-1-like DNase II gene in *Trichinella spiralis*. *Plos Negl Trop Dis.* 2014;8(8):e3097.
58. Wang ZQ, Li LZ, Jiang P, Liu LN, Cui J. Molecular identification and phylogenetic analysis of *Trichinella* isolates from different provinces in mainland China. *Parasitol Res.* 2012;110(2):753–7.
59. Hu X, Liu X, Bai X, Yang L, Ding J, Jin X, Li C, Zhang Y, Li Y, Yang Y, et al. Effects of *Trichinella spiralis* and its excretory/secretory products on autophagy of host muscle cells in vivo and in vitro. *Plos Negl Trop Dis.* 2021;15(2):e0009040.
60. Li Y, Wang B, Zhu Y, Tian Z, Yang Z, Duan J, Wang Z. The cysteine protease ATG4B of *Trichinella spiralis* promotes larval invasion into the intestine of the host. *Vet Res.* 2020;51(1):69.
61. Detwiler C, MacIntyre R. A genetic and developmental analysis of an acid deoxyribonuclease in *Drosophila melanogaster*. *Biochem Genet.* 1978;16(11–12):1113–34.
62. Nadano D, Yasuda T, Kishi K. Measurement of deoxyribonuclease I activity in human tissues and body fluids by a single radial enzyme-diffusion method. *Clin Chem.* 1993;39(3):448–52.
63. Naito Y, Yoshimura J, Morishita S, Ui-Tei K. siDirect 2.0: updated software for designing functional siRNA with reduced seed-dependent off-target effect. *BMC Bioinform.* 2009;10:392.

Publisher's Note

Springer Nature remains neutral with regard to jurisdictional claims in published maps and institutional affiliations.